National Park Service
U.S. Department of the Interior

Science Report NPS/SR—2025/224
https://doi.org/10.36967/2308068

Exploring spatial patterns of overflights at Haleakalā National Park

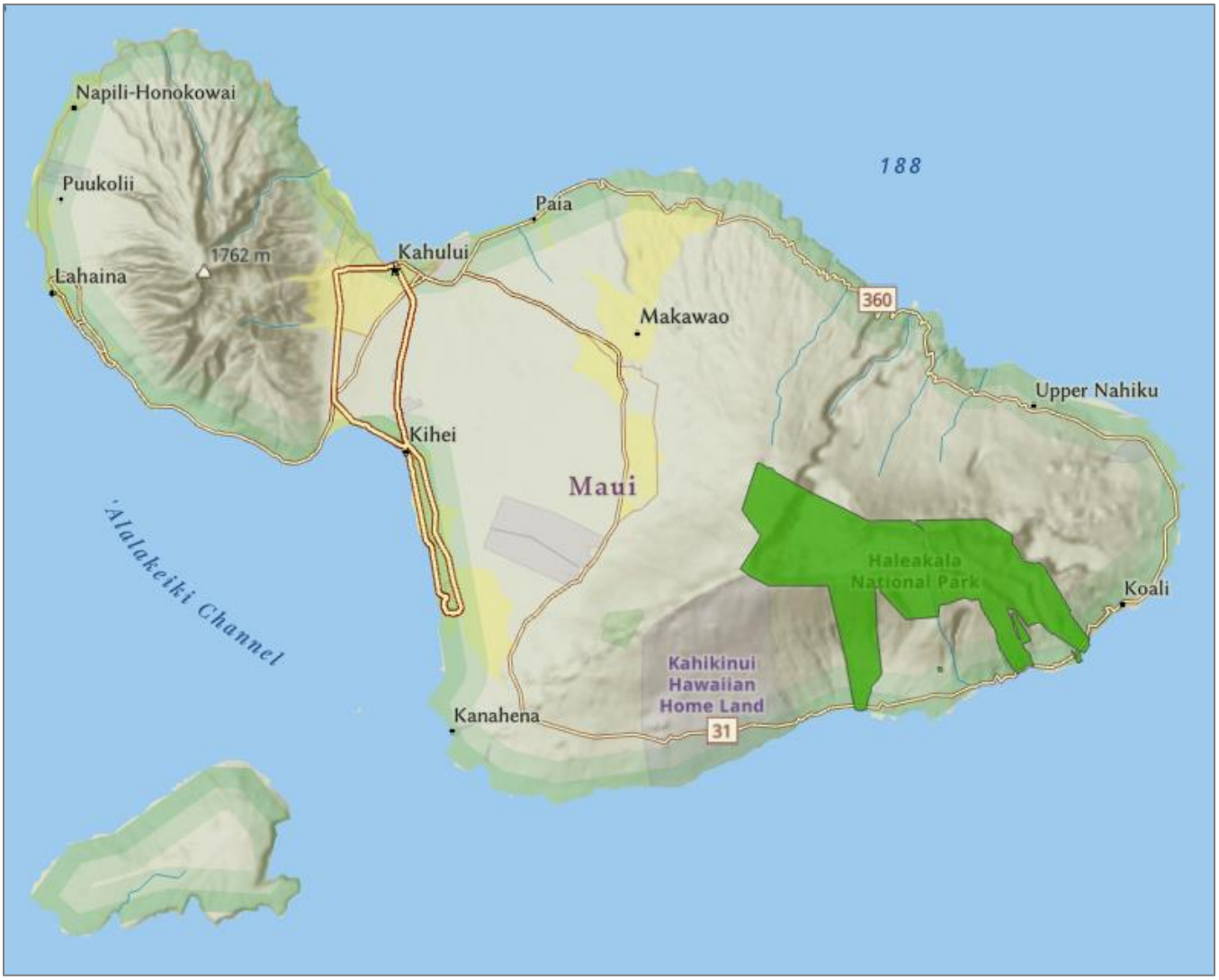

Map of Haleakalā National Park (boundary layer dated 2023).
NPS / BIJAN GURUNG

Exploring spatial patterns of overflights at Haleakalā National Park

Science Report NPS/SR—2025/224

Bijan Gurung[1], J. M. Shawn Hutchinson[1], Brian A. Peterson[1], J. Adam Beeco[2], Sharolyn J. Anderson[2], Damon Joyce[2]

[1] Kansas State University
Manhattan, Kansas

[2] National Park Service
Natural Resource Stewardship and Science
Natural Sounds and Night Skies Division
Fort Collins, Colorado

Please cite this publication as:

Gurung, B., Hutchinson, J. M. S., Peterson, B. A., Beeco, J. A., Anderson, S. J., and Joyce, D. 2025. Exploring spatial patterns of overflights at Haleakalā National Park. Science Report NPS/SR—2025/224. National Park Service, Fort Collins, Colorado. https://doi.org/10.36967/2308068

NPS 162/195906, February 2025

The National Park Service Science Report Series disseminates information, analysis, and results of scientific studies and related topics concerning resources and lands managed by the National Park Service. The series supports the advancement of science, informed decisions, and the achievement of the National Park Service mission.

All manuscripts in the series receive the appropriate level of peer review to ensure that the information is scientifically credible and technically accurate.

Views, statements, findings, conclusions, recommendations, and data in this report do not necessarily reflect views and policies of the National Park Service, US Department of the Interior. Mention of trade names or commercial products does not constitute endorsement or recommendation for use by the US Government.

The Department of the Interior protects and manages the nation's natural resources and cultural heritage; provides scientific and other information about those resources; and honors its special responsibilities to American Indians, Alaska Natives, and affiliated Island Communities.

This report is available in digital format from the National Park Service DataStore and the Natural Resource Publications Management website. If you have difficulty accessing information in this publication, particularly if using assistive technology, please email irma@nps.gov.

Contents

Figures

Page

Tables

Page

Abstract

This study explored spatial patterns of overflights at Haleakalā National Park (HALE). Overflights were analyzed from June 3, 2020, to March 31, 2023, using Automatic Dependent Surveillance-Broadcast (ADS-B) data with a total of 689 days of data. Data were collected using two data loggers that were deployed at Kīpahulu Visitor Center and near Haleakalā Summit. The first phase of analysis focused on all overflights and found a high concentration of overflights along the flight corridors of commercial airlines and recommended air tour routes per the 1998 Letter of Agreement between Haleakalā National Park and the Hawaii Air Tour Association (Maui). The second phase of analysis focused on low-level overflights that fly below 12,500 ft mean sea level (MSL) and are within 10 miles of the HALE boundary. The phase 2 analysis includes six figures based on two seasons and shows a concentration of flights between 6,501–12,500 ft MSL in and around the Summit District and a concentration of flights between 2,501–6,500 ft MSL in and around the Kīpahulu District. The third phase of analysis selected the likely air tours that were flown below 5,000 ft above ground level (AGL) and within 0.5 miles of the HALE boundary. Kernel density analyses were conducted using waypoints segmented into 500 ft above ground level (AGL) altitude intervals from 0–5,000 ft AGL. The altitude interval with the highest density of overflights was 2,501–3,000 ft AGL. Kernel density hot spots were observed above the southern rim of the Haleakalā Crater along the recommended air tour route. The majority of the likely air tours were conducted using rotorcraft and a map displaying their flight pattern is also shown. This information can be used for planning and management purposes, and this study serves as a resource for future research that intends to use more advanced analytics.

Acknowledgements

The authors would like to thank the National Park Service Natural Sounds and Night Skies Division for funding and supporting this project, specifically Vicki Ward, Ashley Pipkin, and Warren Deeds. The authors would also like to thank Joshua Higa from Haleakalā National Park for his support in maintaining the collection units and downloading the data and providing it to us.

List of Acronyms

ADS-B: Automatic Dependent Surveillance-Broadcast

AGL: Above ground level

ATMP: Air Tour Management Plan

DEM: Digital Elevation Model

FAA: Federal Aviation Administration

GIS: Geographic information systems

HALE: Haleakalā National Park

MSL: Mean sea level

NPATMA: National Parks Air Tour Management Act

NPS: National Park Service

Introduction

Haleakalā National Park (HALE) covers more than 33,000 acres on the eastern side of Maui, the second largest island in the state of Hawai‘i, and its wilderness area includes 24,719 acres of land (National Park Service, 2024a). HALE is an international biosphere reserve with an altitude beginning from sea level to the top of Haleakalā volcano at 10,023 ft (Peterson, 2021). The higher elevation area has a volcanic landscape featuring the Alpine Aeolian zone, a barren, porous, rocky, and dry area. The Maui volcano features the large Haleakalā crater at the summit, opening to the northeast and southeast, forming large valleys that extend to the coast. The park includes two districts: the Summit District and Kīpahulu District (Figure 1). The northern and eastern slopes of the Haleakalā crater and the rainforests of Kīpahulu Valley are rich in biodiversity. More than 90% of the native biota found in the Park is endemic to the Hawaiian Islands and 50% is endemic to Maui. The Park is a sacred place to native Hawaiians. An average of 1,050,289 visitors visited annually from 2017 to 2019. The total number of visitors plummeted to 319,147 in 2020 due to travel restrictions imposed during the COVID-19 pandemic but rebounded to 1,087,616 in 2022 (National Park Service, 2024d).

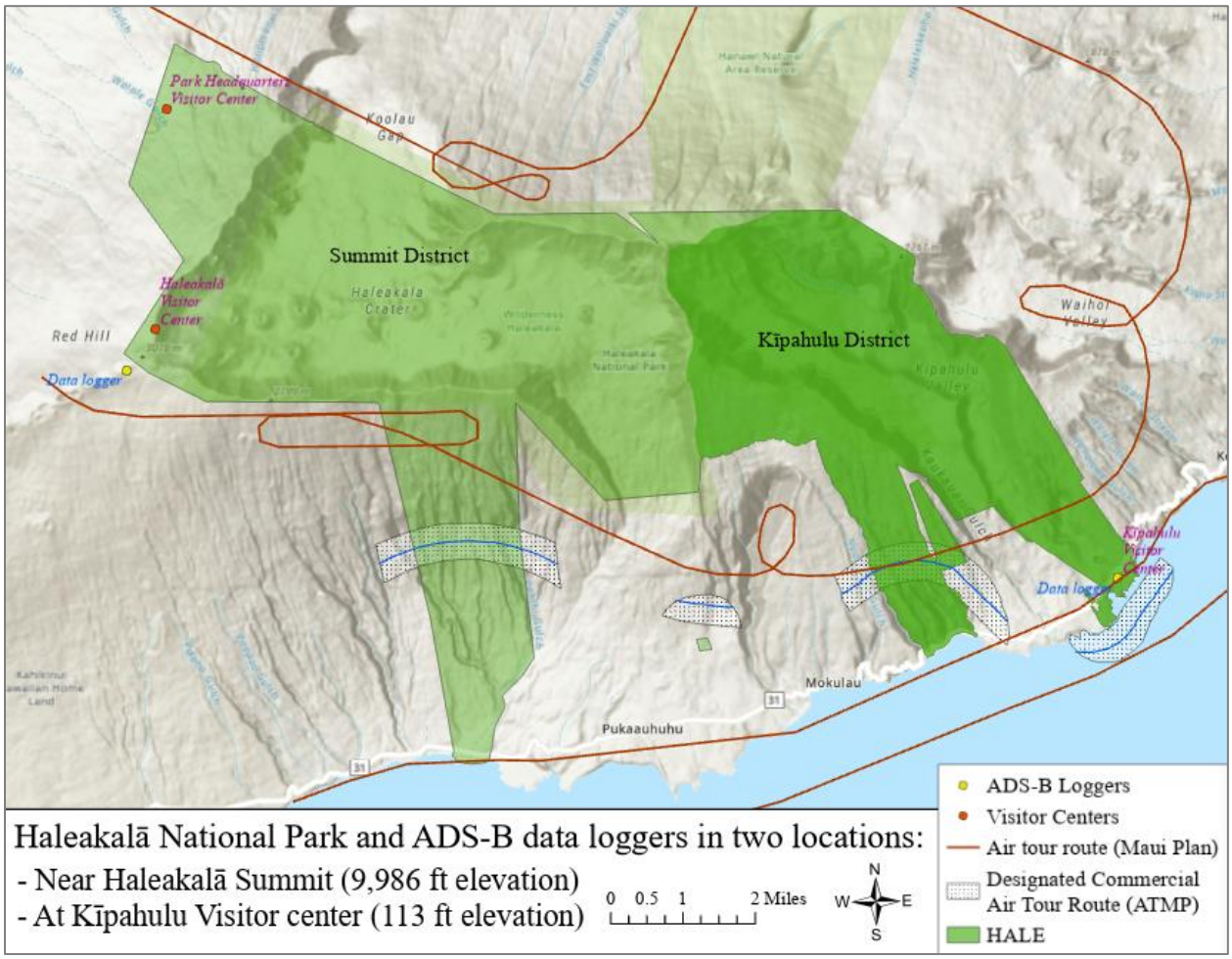

Figure 1. Two locations of ADS-B data loggers. NPS / BIJAN GURUNG

The purpose of this report is to examine the spatial patterns of overflights at HALE.

The National Parks Air Tour Management Act of 2000 (NPATMA) (Public Law 106-81) requires the Federal Aviation Administration (FAA), in cooperation with the National Park Service (NPS), to establish an air tour management plan or voluntary agreement for any park unit whenever someone applies to conduct air tours over the park, except for Grand Canyon National Park and all national parks in the State of Alaska (Beeco & Joyce, 2019). An air tour management plan (ATMP) for HALE was completed in January 2024 by the NPS and the FAA. The plan was designed to protect natural and cultural landscapes and resources, areas of historic and spiritual significance to Native Hawaiians, wilderness characteristics, and visitor experience (National Park Service, 2024a). The plan authorizes a maximum of 2,224 air tours annually that are required to follow a defined route over the park. This number is a 54% reduction from the existing average of 4,824 flights per year (National Park Service, 2024b). This report includes the analysis of datasets collected from 2020 to 2023, just before the implementation of the ATMP. In 1998, prior to the NPATMA, NPS and the Hawaii Air Tour Association executed a Letter of Agreement, also known as Maui Plan, regarding the conduct of air tours over and within the vicinity of HALE; however, compliance with the provisions was voluntary (Beeco et al., 2020; Volpe National Transportation Systems Center, 2004). It is important to understand the travel patterns of commercial air tours and their effect on the acoustic environment of the park.

Using Automatic Dependent Surveillance-Broadcast (ADS-B) data, overflights can be tracked. These data include latitude, longitude, altitude, and unique identification code of the aircraft (Beeco & Joyce, 2019). As of January 1, 2020, the FAA requires all aircraft that enter designated airspace to be equipped with ADS-B technology (see 14 CFR § 91.225 and 14 CFR § 91.227). HALE is located under uncontrolled airspace, which means ADS-B is not required on aircraft that fly above HALE. The nearest airport, Kahului Airport, is Class B airspace and ADS-B is required to access this airspace.

Two data loggers were deployed at two sites: near the summit of Haleakalā and Kīpahulu Visitor Center. Data were collected from June 3, 2020, to March 31, 2023, but there were gaps in the data recording days with a total of 689 days of data recording. The data captured 70,524 overflights. After selecting the overflights below 5,000 ft AGL and within the 0.5-mile boundary of the park, the dataset was comprised of 4,098 low-level overflights mostly representing commercial air tours.

Methods

Data Collection

Data were collected by two ADS-B terrestrial data loggers located at Kīpahulu Visitor Center (20.661578 N, -156.04495 W; 91 ft MSL) and near Haleakalā Summit (20.706988 N, -156.255991 W; 9,968 ft MSL) (Figure 1). The former is located within the park boundary, while the latter is slightly outside but within a 0.5-mile distance of it. The data loggers were positioned with an unimpeded and expansive skyward exposure. The loggers recorded ADS-B signals as text files (TSV). The data logger placed at Kīpahulu Visitor Center captured ADS-B data from June 3, 2020, to September 9, 2021, with 260 days of data recorded. The data logger placed near Haleakalā Summit recorded ADS-B data from September 1, 2020, to March 31, 2023, with 599 days of data recorded. Both dataloggers were recording ADS-B data simultaneously..

Data Processing and Cleaning

Data processing, cleaning, and analysis were accomplished using a custom ArcGIS Pro toolbox with multiple Python-based geoprocessing tools that automated and simplified the processing and analysis of ADS-B data (Hutchinson & Peterson, 2023). The toolbox conducted the following tasks: processed raw ADS-B data files, removed repeated occurrences of waypoints (duplicate records) collected by data loggers, created waypoint and flightline feature classes, merged daily waypoints and flightlines, screened waypoints and flightlines, summarized waypoint altitudes, summarized the number of flights across several temporal scales (monthly, daily, hourly), and summarized number of flights across aircraft types (rotorcraft, fixed wing single engine, fixed wing multi engine).

This report expresses altitude using mean sea level (MSL) and above ground level (AGL). Altitude expressed in MSL refers to the altitude of an aircraft above sea level, regardless of the terrain below it, whereas altitude expressed in AGL is a measurement of the distance between the ground surface and the aircraft. To calculate AGL altitudes for each waypoint, a 10-meter digital elevation model (DEM) was used (United States Geological Survey, 2023). The AGL altitudes were calculated by subtracting the elevation of the DEM from the reported altitudes of the ADS-B logger (z-coordinate) for every point location (x, y) (see Beeco et al., 2020 for the exact method).

ADS-B technology can use either barometric altitude or geometric altitude. Barometric altitude is determined by measuring air pressure and must be regularly calibrated. Geometric altitude is calculated using the Global Positioning System (GPS). While errors can result from each type of technology, GPS is generally considered a more reliable and accurate measure; however, the aviation industry has long used barometric altitudes during flight. Aircraft owners and operators determine which system to use on their aircraft. The analysis in this report does not attempt to correct any errors associated with altitude information, as this would be nearly impossible and overly burdensome. Therefore, calculations of AGL altitudes can in some cases be negative. This can occur for low-flying aircraft that have an ADS-B system reporting an altitude lower than the actual altitude. Negative AGL altitude calculations can also be due to an aircraft's ADS-B system malfunction. Further, AGL is calculated using 10 m x 10 m Digital Elevation Models (DEM). This level of resolution can also introduce errors. Negative AGL values are reported in the analysis. Finally, in

some datasets, MSL altitudes in the data are also negative. This is likely due to a system error. These data generally represent less than 0.1% of the total data and are discarded from the analysis.

To explore spatial patterns of overflights at HALE, analyses were conducted in three phases. Phase 1 and Phase 2 report altitudes using MSL, while Phase 3 uses AGL. MSL is better suited for understanding aircraft patterns across a larger space or scale because the baseline (mean sea level) does not change. However, AGL analysis was used because Phase 3 includes more detailed examinations of the data and thus, this analysis better contextualizes the proximity of aircraft above undulating terrain and associated terrestrial resources and visitors' experiences. All maps produced during analysis used Esri basemaps with service layer credits for: Esri, USGS, Washington Game Fish and Parks, HERE, Garmin, SafeGraph, FAO, METI/NASA, EPA, and NPS; additionally, all data were projected to North American Datum 1983 Universal Transverse Mercator Zone 4N.

Phase 1 Methods

The purpose of the first phase was to explore all overflight paths above HALE regardless of flight type or altitude. Thus, the flightline feature class was not cleaned of any flight types, nor was an altitude threshold implemented. To understand how flight paths extended beyond the park boundary, a 10-mile buffer around the HALE boundary was used. One map was produced that shows all overflights during the data collection period from June 3, 2020, to March 31, 2023.

Phase 2 Methods

The purpose of the second phase was to understand low-level overflights above HALE regardless of flight type. Similar to Phase 1, a 10-mile buffer was used. Low-level overflights were defined as having an altitude of less than 12,500 ft MSL. This altitude was chosen because the highest point at HALE is 10,023 ft (National Park Service, 2024c), and approximately 2,500 ft above this point would capture flights that have the greatest impact on the acoustic environment within the park. To understand flight altitudes, a waypoint feature class was used. Six maps were produced (across seasons) that show all overflights that flew beneath 12,500 ft MSL and within 10 miles of HALE. These maps classified waypoints using MSL altitudes. There are two seasons in Hawai‘i: summer (kau) from May to October and winter (ho‘oilo) from November to April.

Phase 3 Methods

The purpose of the third phase was to focus on flights that are likely commercial air tours. The toolbox joined ADS-B data to the FAA Releasable Database via aircraft unique identifiers (e.g., ICAO address) to determine aircraft tail number, type registrant (e.g., government), type aircraft, engine type, model, and owner's name. This information was applied in the ADS-B toolbox to screen the suspected flights known not to be air tours by: 1) cleaning the data of civil patrol flights, 2) major airlines, 3) straight-line flights, 4) flights with a flightpath less than a mile in length, and 5) survey flights. Civil patrol flights were identified as government aircraft (FAA releasable database type registrant = 5). Major airlines were identified such as American Airlines, Delta Airlines, SkyWest Airlines, Southwest Airlines, Hawaiian Airlines, Alaska Airlines, and United Airlines. Straight-line flights were screened by calculating their sinuosity values. Sinuosity measures the meandering of a path from the straight-line condition and is calculated as the ratio of total flight path length to the

straight-line distance from the flight's initial and final waypoints. A perfectly straight flight path would have a sinuosity of one, but as the number of meanders in the path increases (e.g., the characteristic back-and-forth of survey flight behavior), sinuosity will begin to approach zero. All overflights with sinuosity values greater than or equal to 0.80 were subsequently removed from the analysis. Flights that were less than a mile in length were removed due to data integrity issues. Lastly, survey flights were removed from the analysis because of their undue influence on analysis, infrequent nature, and known flight purpose. Survey flights were identifiable by their flight patterns (parallel patterns by moving back and forth). These survey flights were visually inspected or identified and removed. Meanwhile, air tour behavior generally consists of flight routes that veer toward sightseeing locations and consist of sporadic S-turns and loops (Beeco & Joyce, 2019). After these cleaning steps, the remaining flights are likely air tours, but they have to be cross-checked for confirmation.

A point density analysis was conducted for the waypoints within the 0.5-mile buffer around the park and below 5,000 ft AGL. Similarly, using a 500 ft AGL altitude interval, waypoint data were segmented into the following categories: 0–500 ft AGL; 501–1,000 ft AGL; 1,001–1,500 ft AGL; 1,501–2,000 ft AGL; 2,001–2,500 ft AGL; 2,501–3,000 ft AGL; 3,001–3,500 ft AGL; 3,501–4,000 ft AGL; 4,001–4,500 ft AGL; and 4,501–5,000 ft AGL. Kernel density analysis was then conducted for each altitude interval. Since each altitude interval had different amounts of waypoints, density classifications were normalized across altitude intervals. To do this, the altitude interval with the highest maximum density of waypoints (2,501–3,000 ft AGL) was used to normalize density classification, which required two steps. First, the 2,501–3,000 ft AGL altitude density was classified using equal interval percentage breaks with five intervals of 20%. These percentage breaks were determined using the maximum number of waypoints per square kilometer as the '100%' value. Second, the maximum number of waypoints per each 20% interval was then applied to density classifications for the other altitude intervals. These steps are necessary to ensure that density is calculated the same across altitude intervals regardless of the number of waypoints.

The kernel density analyses produced two main figures. The first figure showed density analysis across sequential altitude intervals (beginning with the lowest altitude interval) from 0–5,000 ft AGL. The second figure showed zoomed-in maps of the density hot spots for 2,501–3,000 ft AGL altitude interval. Similarly, a third figure was generated for 2,001–2,500 ft AGL altitude interval which had the second highest density in kernel density analysis. After these steps were accomplished, kernel density outputs were statistically compared for relatedness using the 'Band Collection Statistics' tool which conducted a spatial correlation test.

Figures were produced to spatially compare the AGL and MSL waypoint trends. The first figure displayed waypoint altitudes ranging from 0 to 5,000 ft AGL, using a 500 ft AGL interval. The second figure displayed waypoint altitudes ranging from 0 to 12,500 ft MSL, using a 1,000 ft MSL interval. Similarly, another figure was produced that shows the waypoints altitudes less than 0 ft AGL.

Descriptive analyses were conducted to understand waypoint frequencies across AGL and MSL altitudes; the number of flights across months, days of the week, and hours of the day; and the number of flights across aircraft types. To gain insight into overflight travel patterns across aircraft types, three more figures were produced for rotorcraft, fixed wing single engine aircraft, and fixed wing multi engine aircraft.

Results

Results – Phase 1

Two data loggers were deployed: one at Kīpahulu Visitor Center and one near Haleakalā Summit (Figure 1). Data were collected from June 3, 2020, to March 31, 2023. There was a gap in data recording from July 29, 2022, to December 22, 2022. There was also a gap after January 2022 that lasted for more than a month. Figure 1 shows the locations of the data loggers, visitor centers, park districts, recommended air tour routes (from the Maui Plan), and designated air tour routes in the ATMP. Figure 2 displays the travel patterns of all overflights above HALE (n = 70,524). Visual analysis of these data suggests some flight paths or flight corridors of commercial airlines and flights similar in pattern to the recommended air tour route in the 1998 Maui Plan.

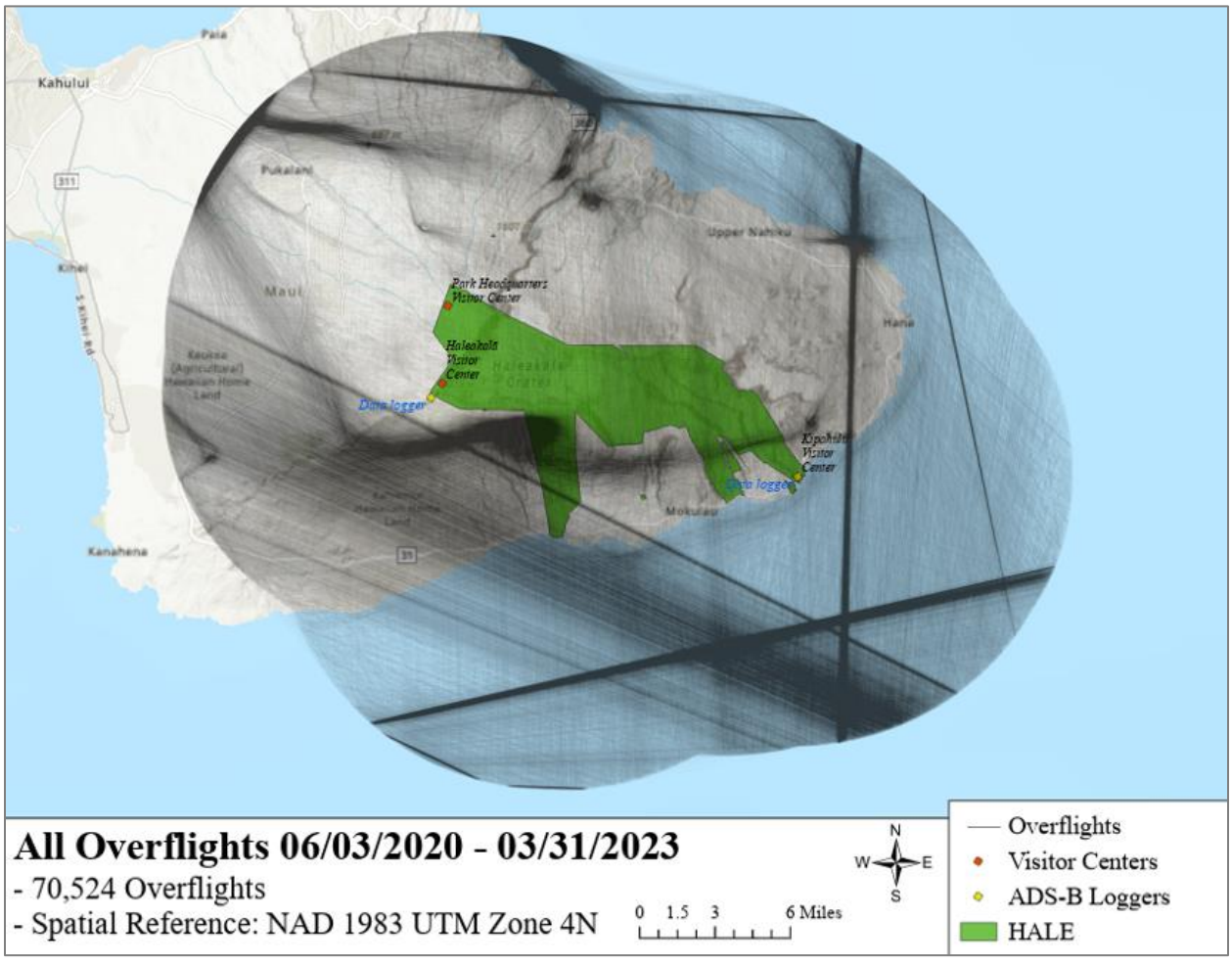

Figure 2. Overflights between June 3, 2020 and March 31, 2023. NPS / BIJAN GURUNG

Results – Phase 2

Waypoints of low-level overflights that flew below 12,500 ft MSL and within a 10-mile buffer around the park regardless of flight type were mapped, which included 6,415,984 waypoints (13,225

overflights). Six figures were produced for winter (November–April) and summer seasons (May–October). Figure 3 shows waypoint MSL altitudes for June 3, 2020, to October 31, 2020. Figure 4 shows waypoint MSL altitudes for November 1, 2020, to April 30, 2021. Figure 5 shows waypoint MSL altitudes for May 1, 2021, to October 31, 2021. Figure 6 shows waypoint MSL altitudes for November 1, 2021, to April 30, 2022, where parallel patterns of survey flights are evident. Figure 7 shows waypoint MSL altitudes for May 1, 2022, to July 29, 2022, but contains only 10 days of data. There was no data after July 29, 2022, until December 22, 2022, so the density of waypoints is quite low in Figure 7. Figure 8 shows waypoint MSL altitudes for December 22, 2022, to March 31, 2023.

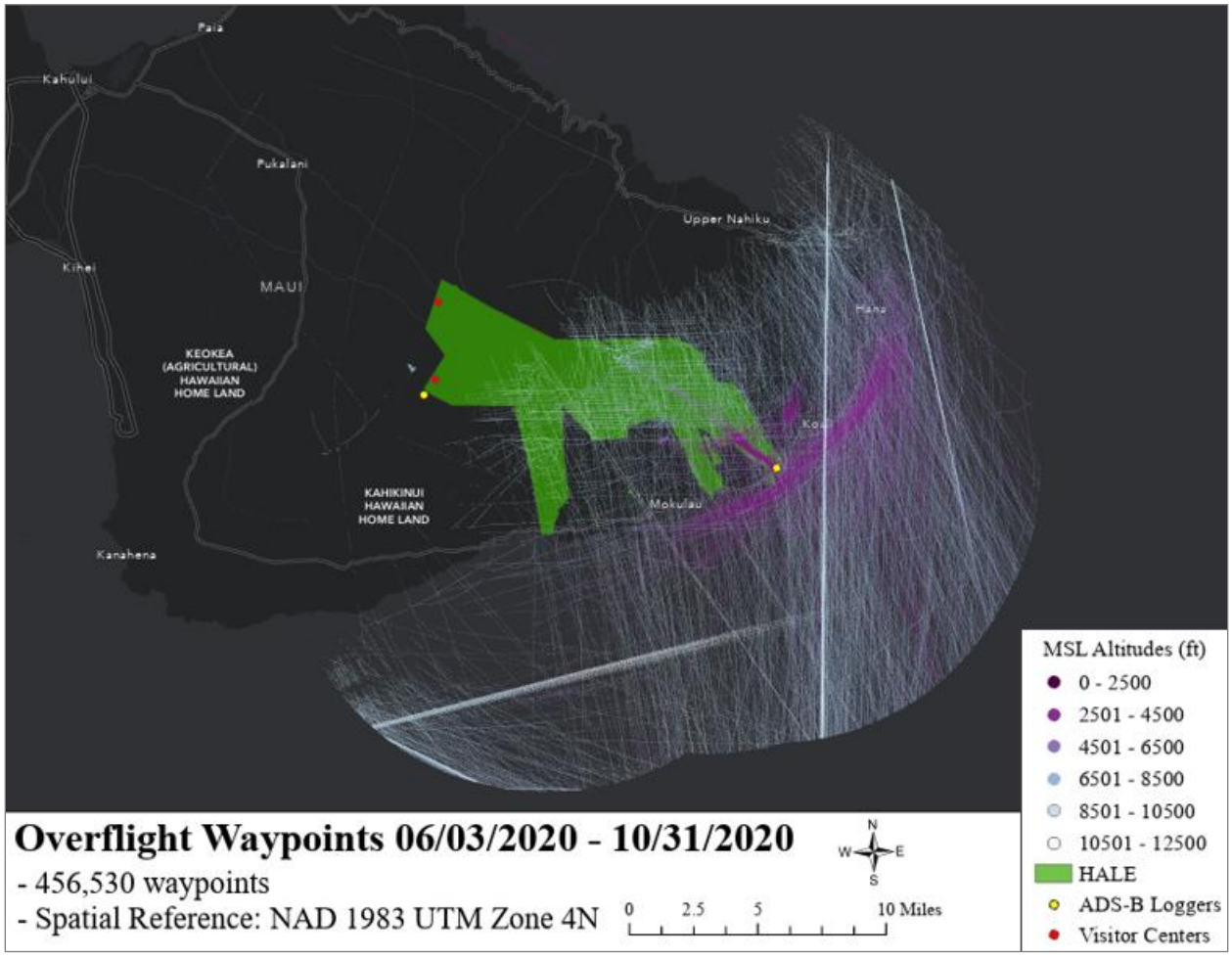

Figure 3. Waypoint MSL altitudes for June 3, 2020, to October 31, 2020 (summer–five months). Data were collected from mostly the Kīpahulu unit during this period. NPS / BIJAN GURUNG

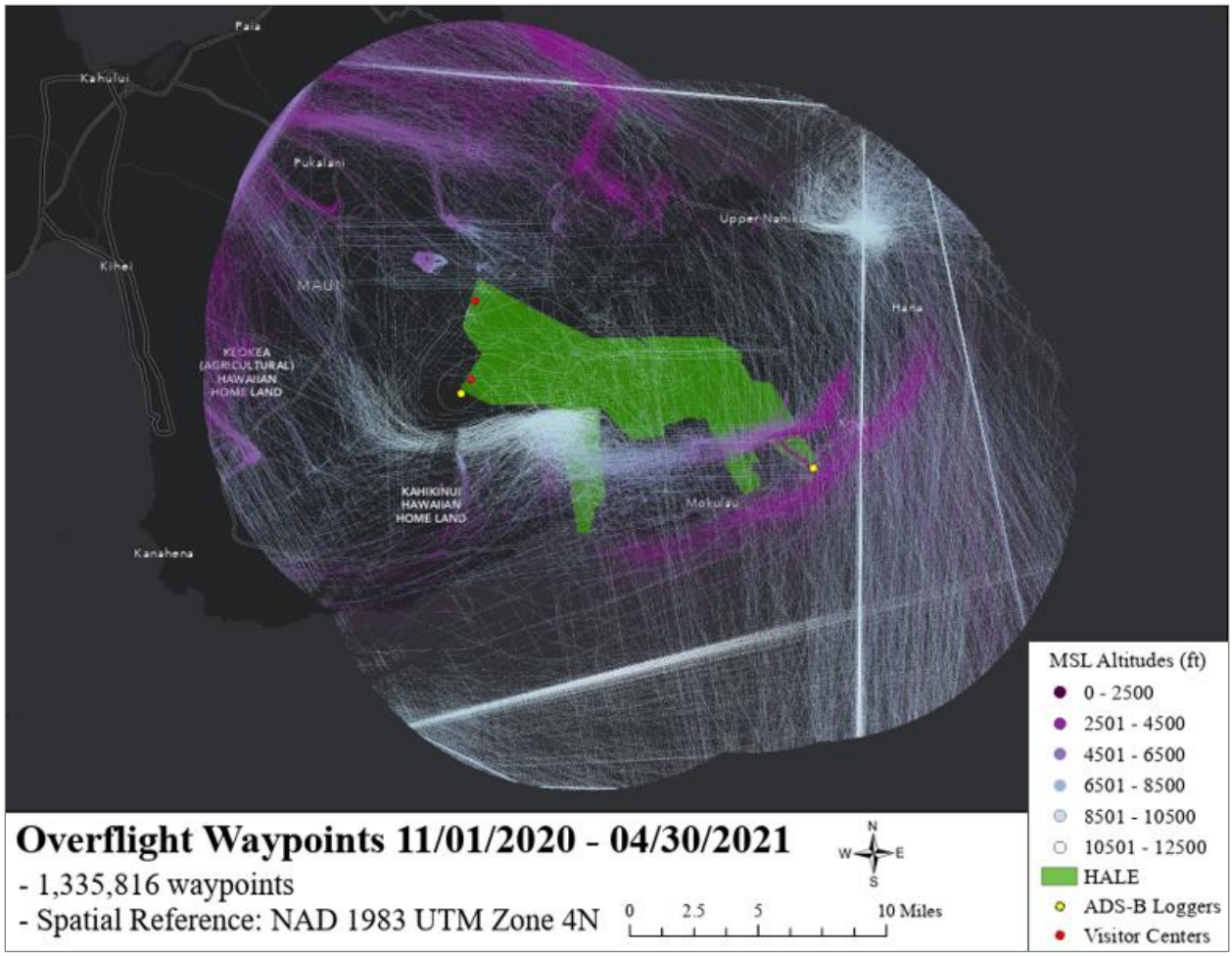

Figure 4. Waypoint MSL altitudes for November 1, 2020, to April 30, 2021 (winter–six months). Data were collected from both units during this period. NPS / BIJAN GURUNG

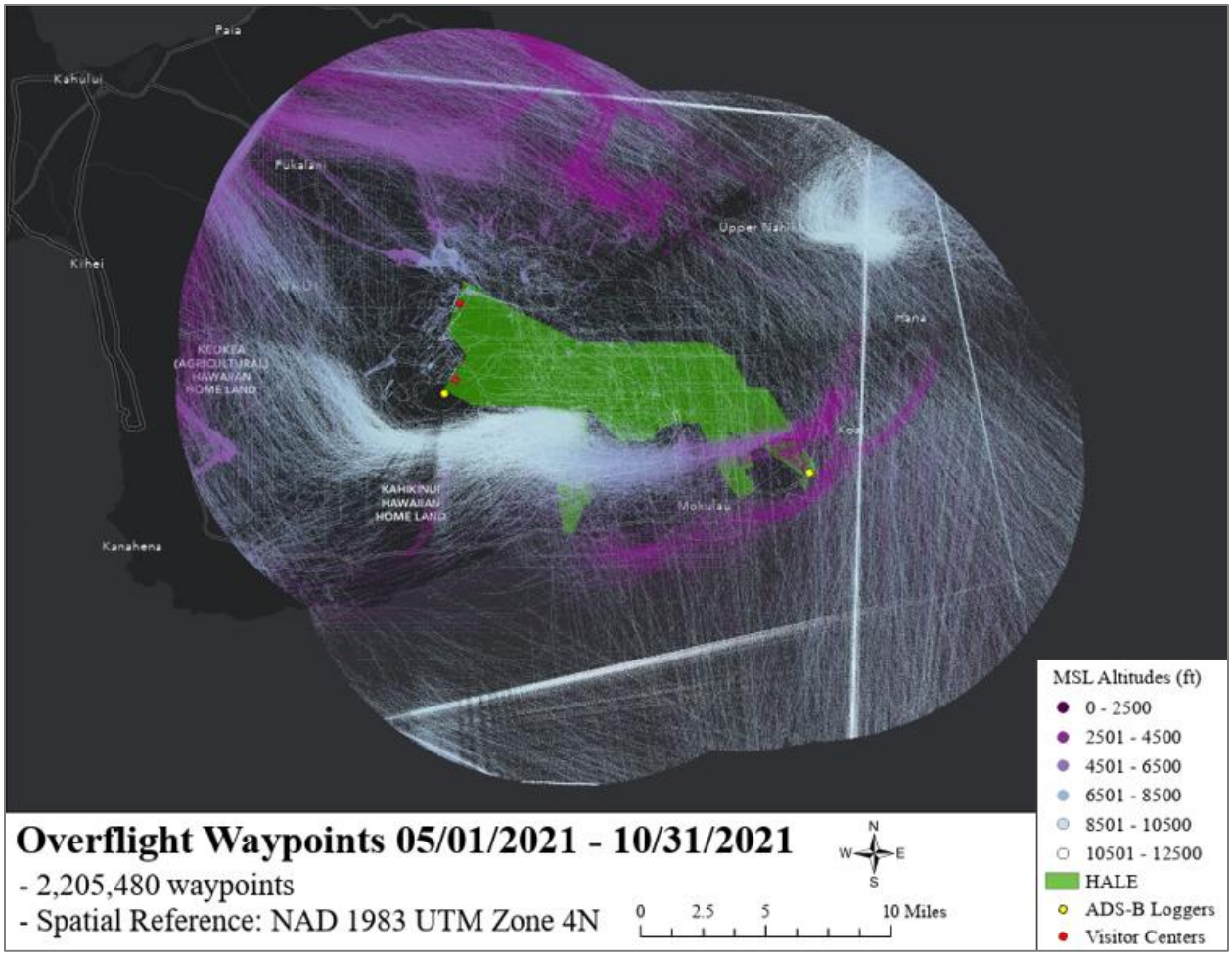

Figure 5. Waypoint MSL altitudes for May 1, 2021, to October 31, 2021 (summer–six months). Data were collected from both units during this period. NPS / BIJAN GURUNG

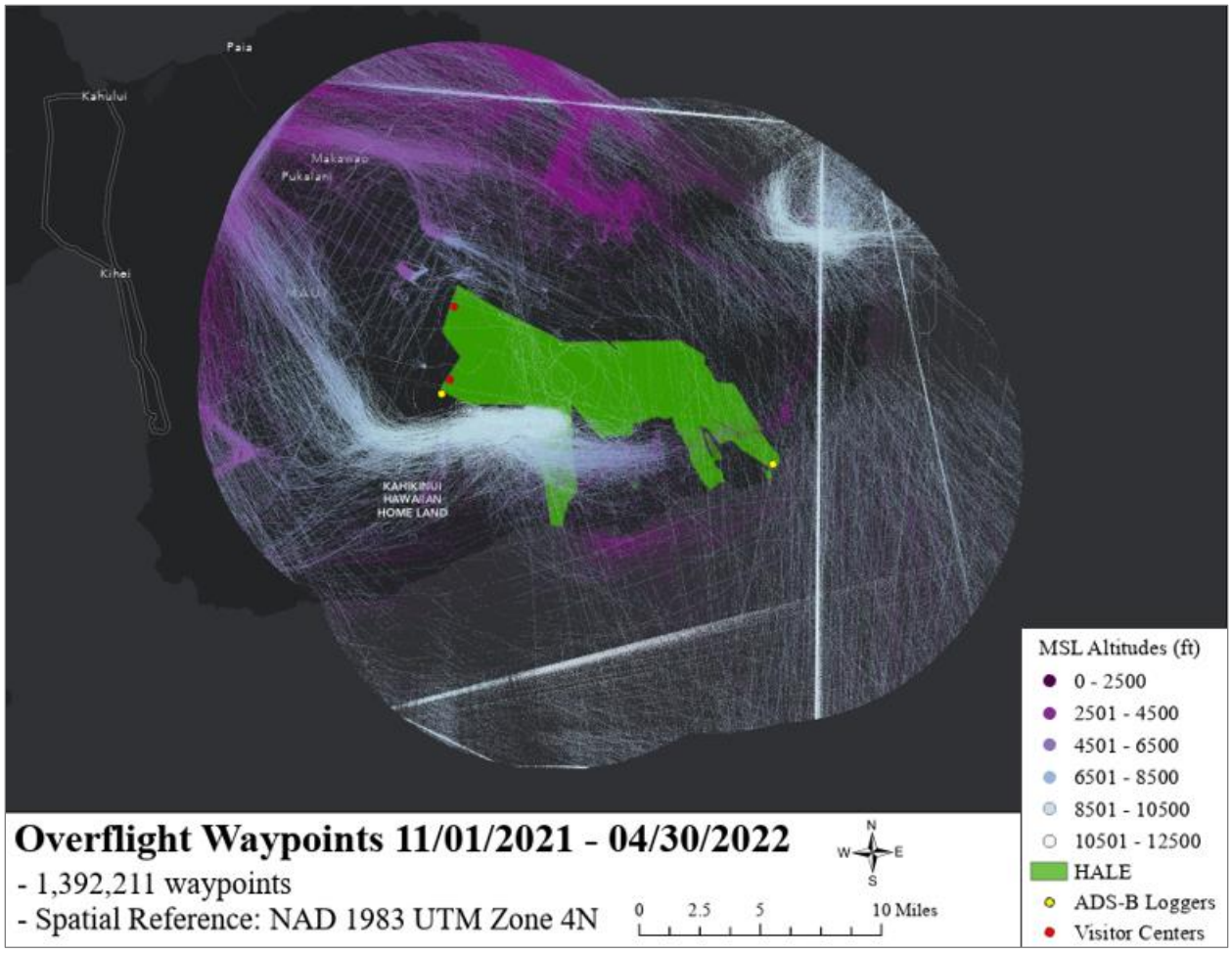

Figure 6. Waypoint MSL altitudes for November 1, 2021, to April 30, 2022 (winter–six months). Data were collected from only the summit unit during this period. NPS / BIJAN GURUNG

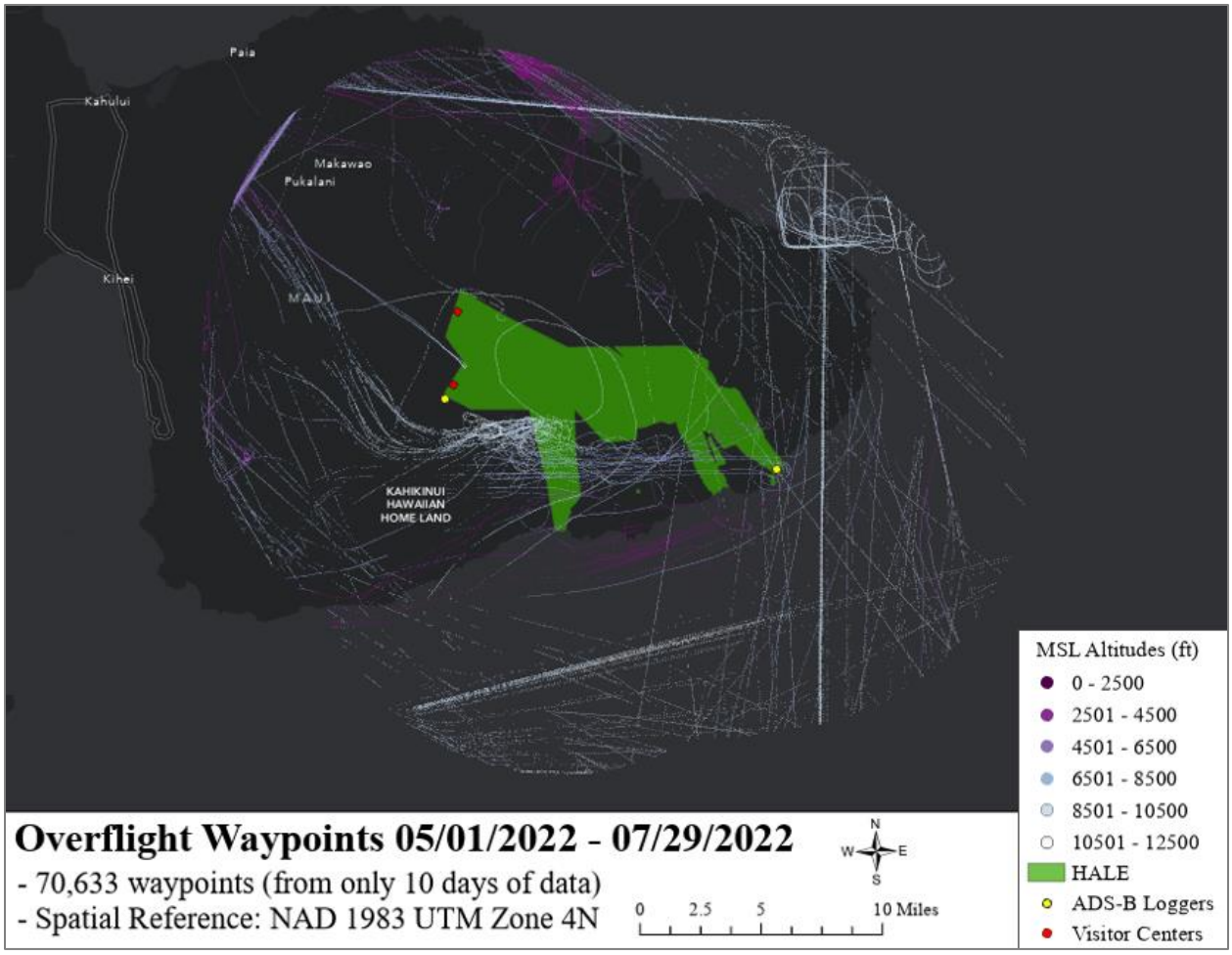

Figure 7. Waypoint MSL altitudes for May 1, 2022, to July 29, 2022 (summer–10 days of data). Data were collected from only the summit unit during this period. NPS / BIJAN GURUNG

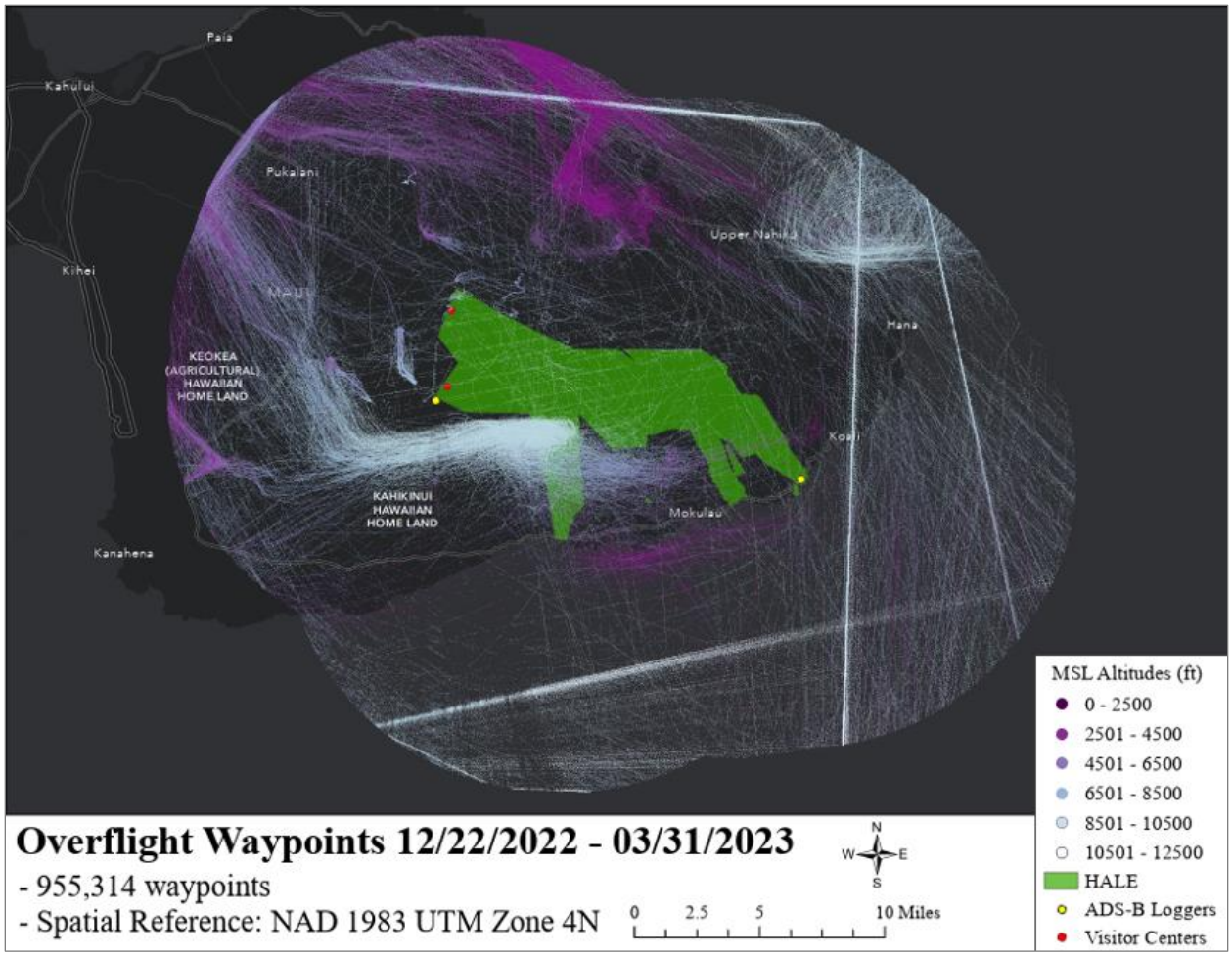

Figure 8. Waypoint MSL altitudes for December 22, 2022, to March 31, 2023 (winter–slightly more than three months). Data were collected from only the summit unit during this period. NPS / BIJAN GURUNG

Results – Phase 3

Phase 3 included the analysis of flights representing likely air tours. Data were cleaned of all flights that were not likely air tours based on the criteria described in the methods. The following number of flights were removed: 21 civil patrol flights, 60,599 straight-line flights, 278 major airlines' flights, 460 flights with a flight path less than a mile in length, and 46 survey flights. This left 9,095 flights for phase 3 analysis.

Figure 9 displays the Phase 3 data along with the voluntary route. Variances between the route and the aircraft tracks exist primarily in two places. South of the loop in the west of the park, aircraft tracks existed in abundance. The second location of discrepancies is on the east of the park where aircraft tracks are mostly north of the voluntary route. A point density analysis was conducted for the waypoints below 5,000 ft AGL and within the 0.5-mile boundary of the park (Figure 10). The density image was laid over the waypoints to improve comparison and visualization of the results. A high density of waypoints was observed above the southwestern side of the park, just south of the crater rim, where the loop on the voluntary route is located.

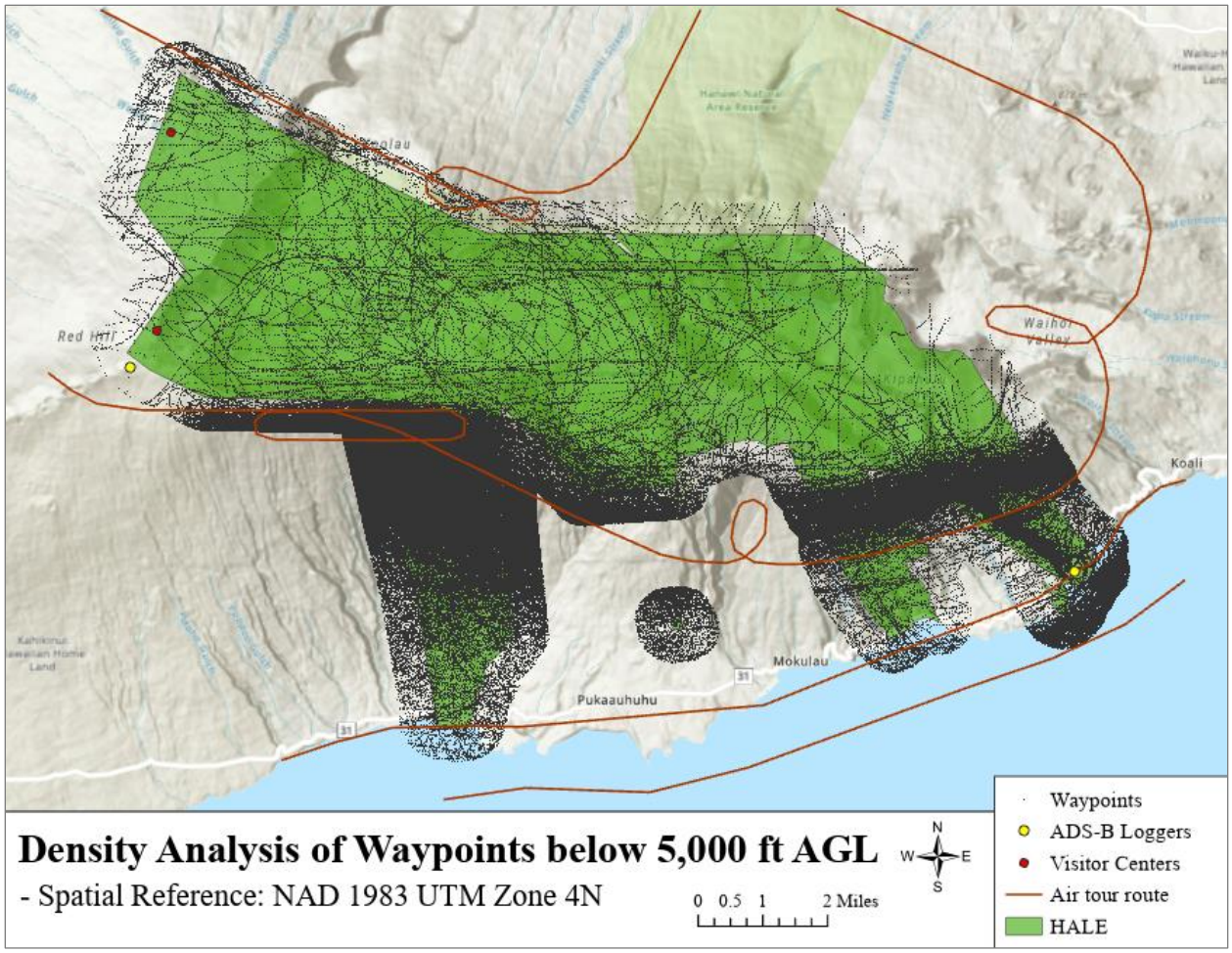

Figure 9. All waypoints below 5,000 ft AGL and with 0.5-mile buffer around the park.
NPS / BIJAN GURUNG

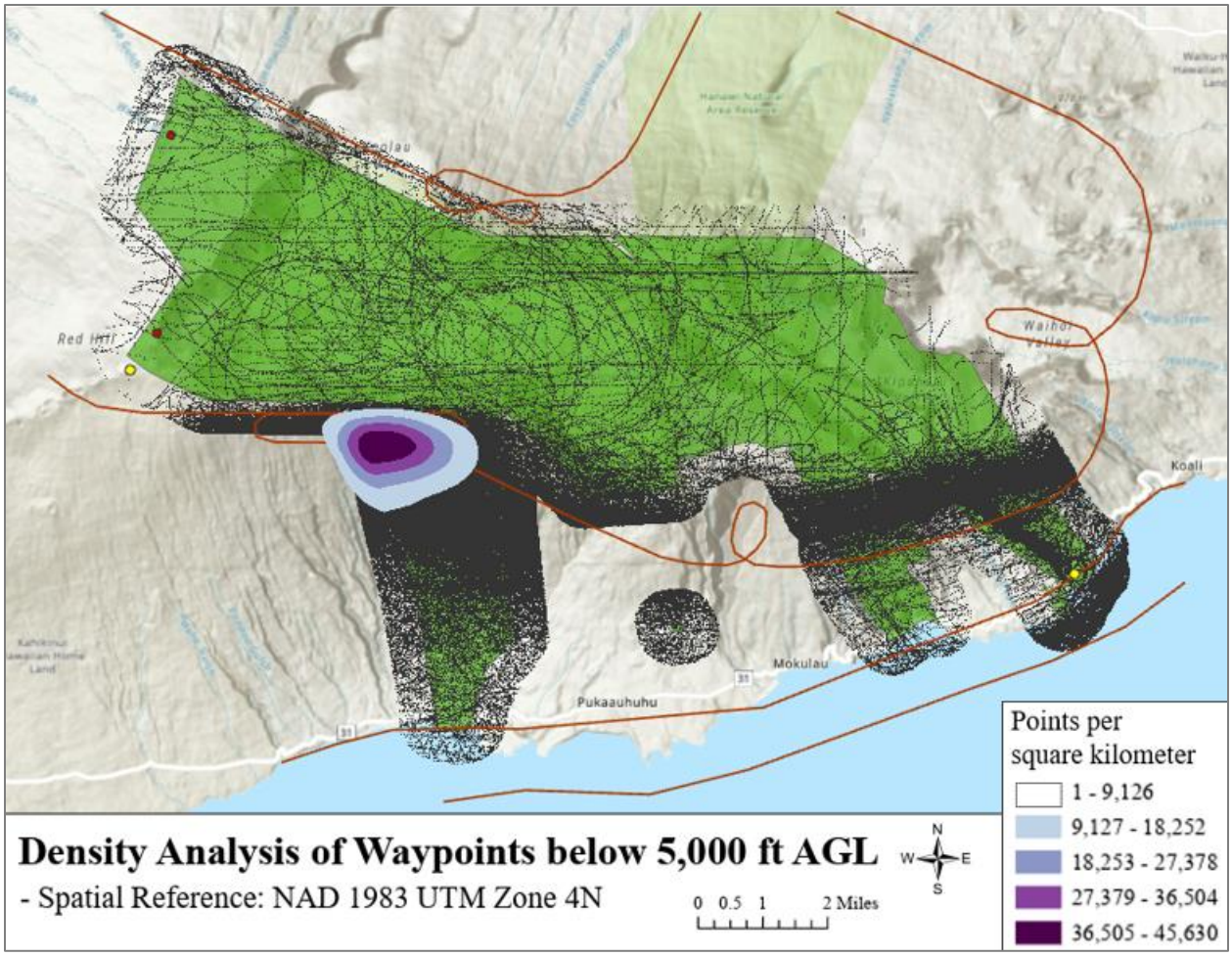

Figure 10. Density Analysis of waypoints lying below 5,000 ft AGL. NPS / BIJAN GURUNG

Similarly, kernel density analysis was conducted for the waypoints in each AGL altitude category from 0–500 ft AGL to 4,501–5,000 ft AGL at 500 ft intervals. Kernel density analysis is based on a kernel function or a probability density function of a random variable (also known as tapering function), which is zero-valued outside of some chosen interval, normally symmetric around the middle of the interval, usually near a maximum in the middle, and usually tapering away from the middle. The AGL altitude interval that showed the most density was 2,501–3,000 ft AGL. The second highest density was observed in the AGL altitude interval of 2,001–2,500 ft. Figure 11 shows the kernel density hot spots for 0–2,500 ft AGL altitudes and Figure 12 shows the kernel density hot spots for 2,501–5,000 ft AGL altitudes. At lower AGL altitudes, density hot spots are observed above the southeastern side of the park or above Kīpahulu area which has several waterfalls. There is no density hot spot for 1,001–1,500 ft AGL altitude interval. Higher density hot spots are observed above the southwestern side of the park, south of Haleakalā Crater from the AGL altitude interval of 1,501–2,000 ft to 4,501–5,000 ft. The highest density hot spots are observed from 2,001–2,500 ft AGL altitude interval to 3,001–3,500 ft AGL altitude interval.

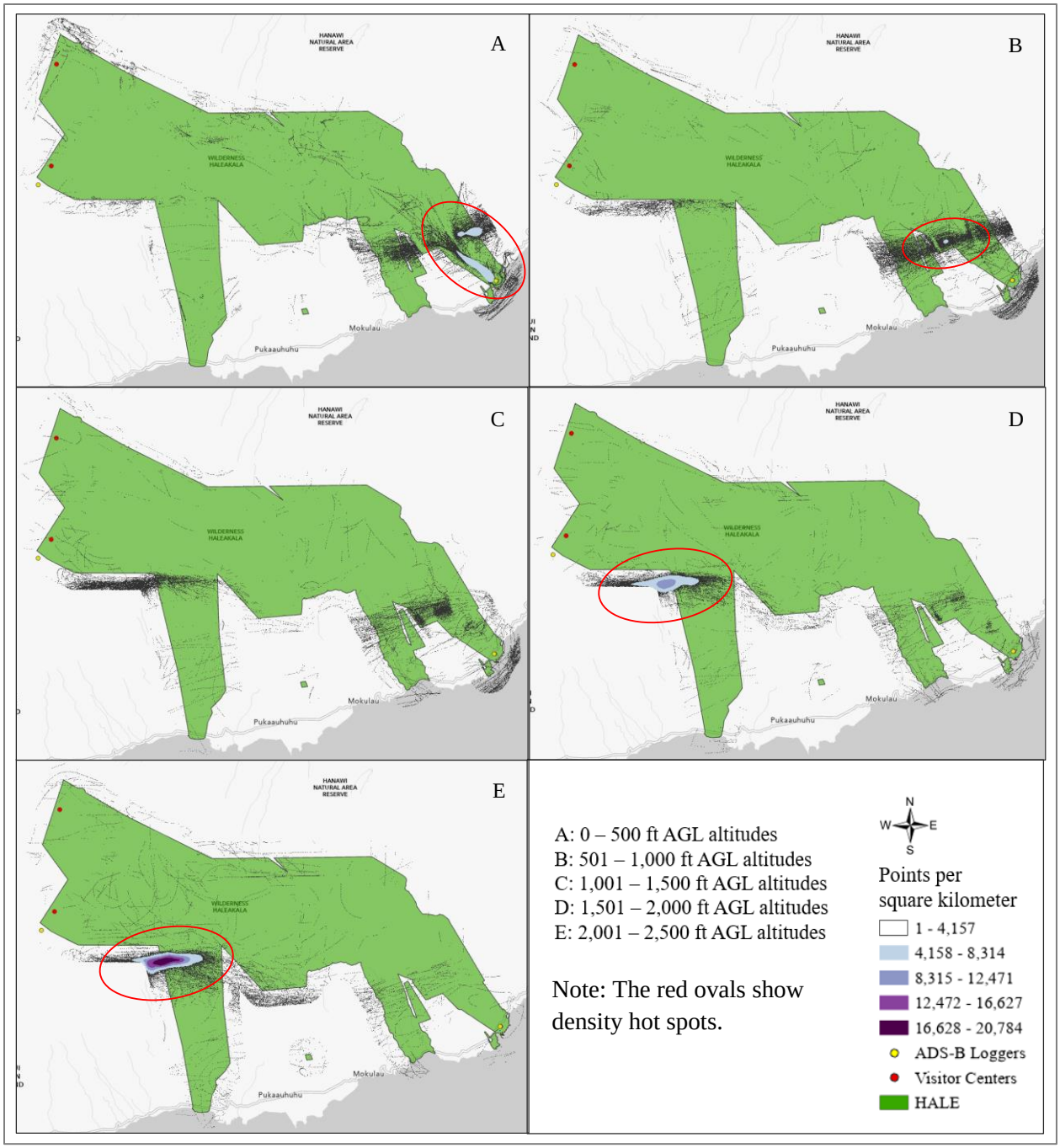

Figure 11. Kernel density across AGL altitudes ranging from 0 to 2,500 ft AGL. NPS / BIJAN GURUNG

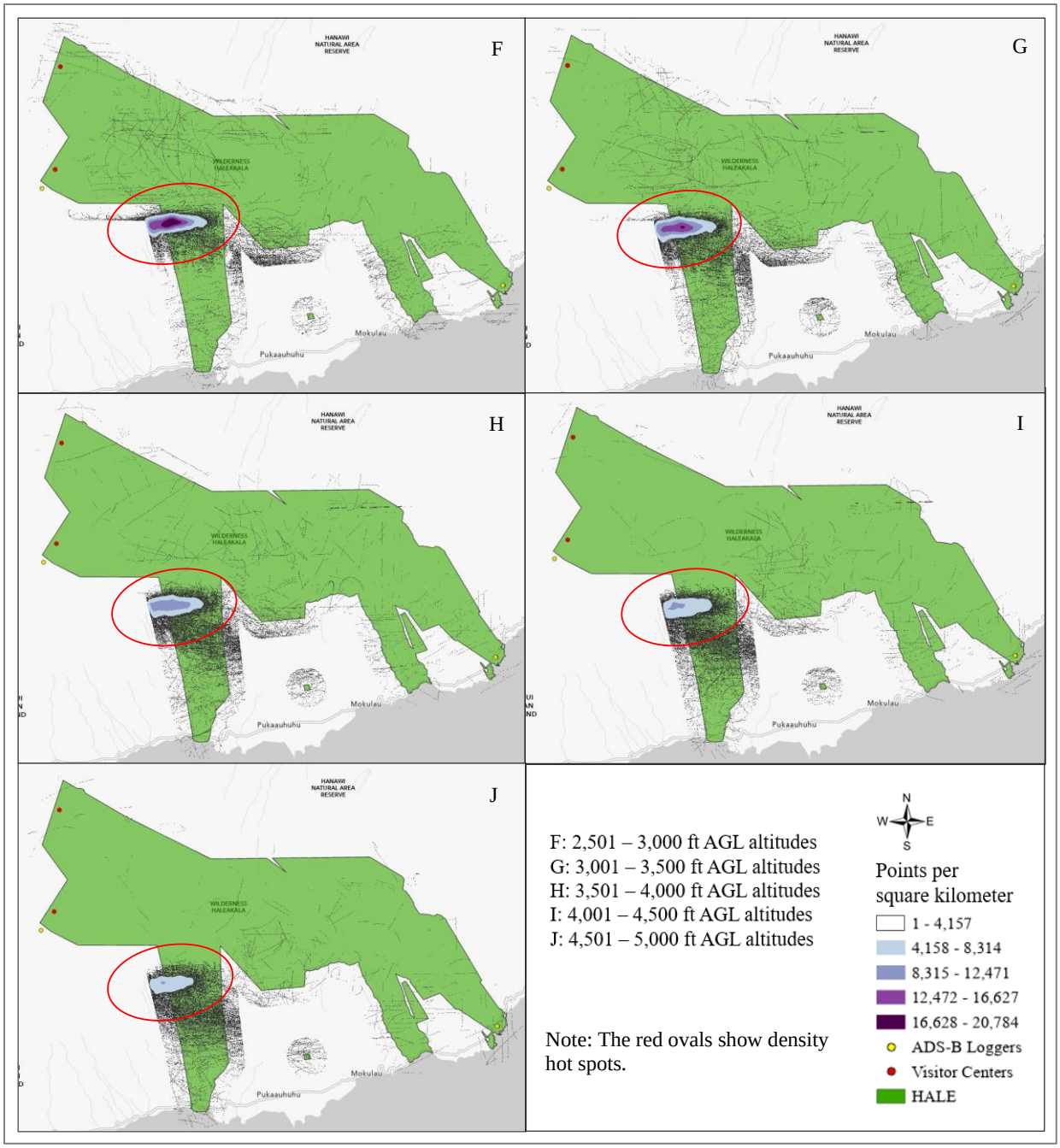

Figure 12. Kernel density across AGL altitudes ranging from 2,501 to 5,000 ft AGL.
NPS / BIJAN GURUNG

The AGL altitude interval with the highest density of waypoints is shown in Figure 13. The AGL altitude interval with the second highest density of waypoints is shown in Figure 14.

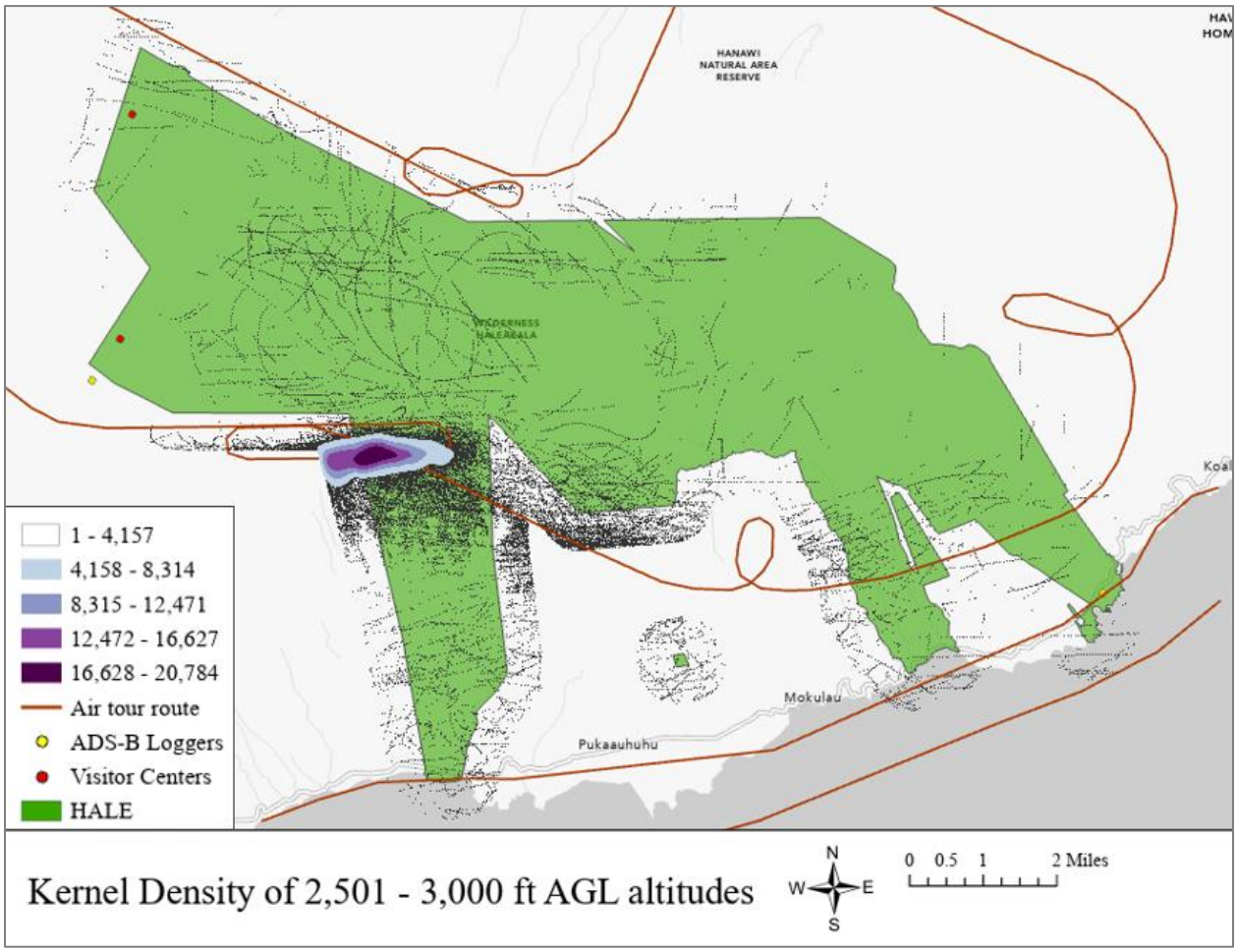

Figure 13. Kernel density image of 2,501–3,000 ft AGL altitude. NPS / BIJAN GURUNG

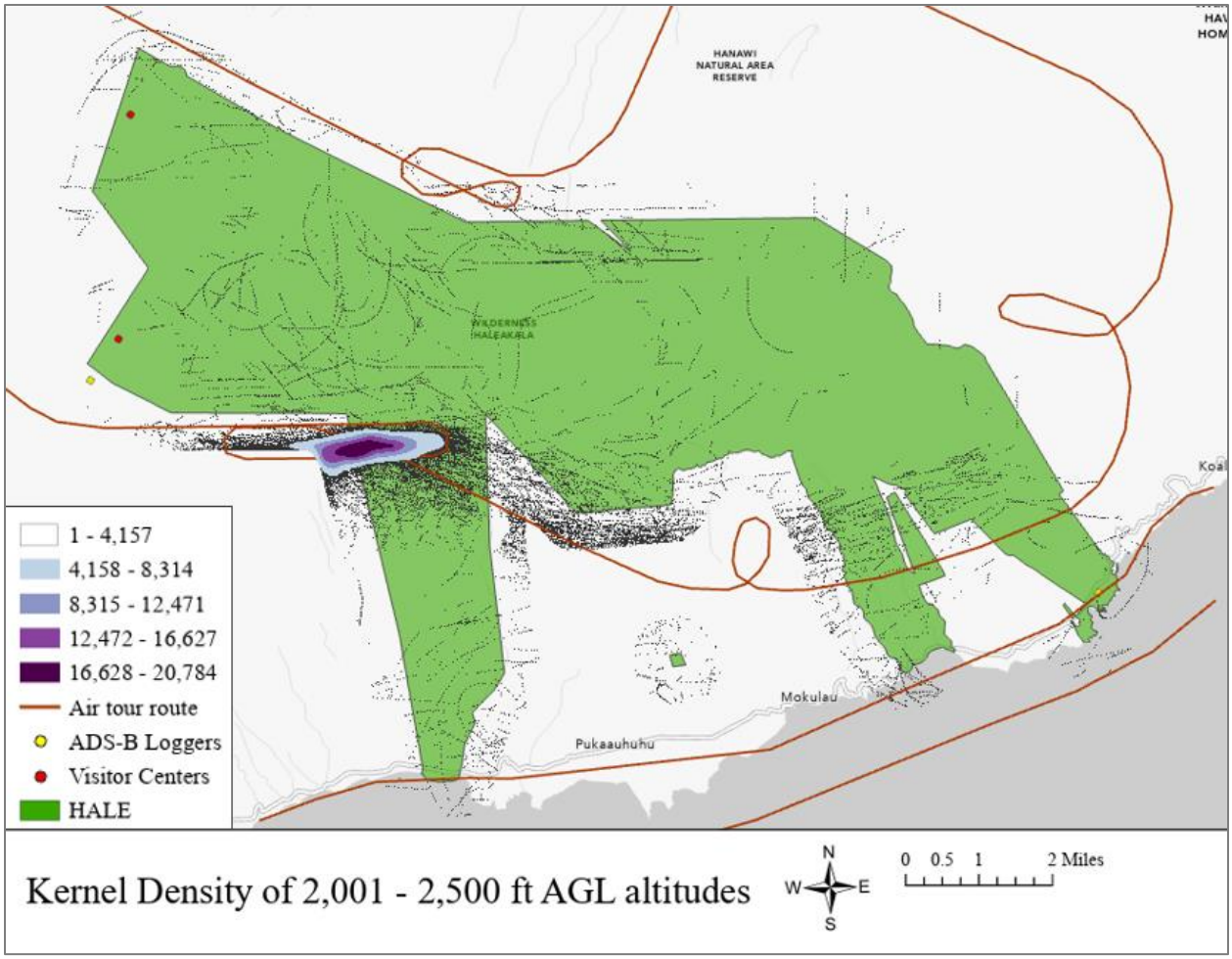

Figure 14. Kernel density image of 2,001–2,500 ft AGL altitude. NPS / BIJAN GURUNG

The correlation coefficients of ten density output or raster images were calculated (Table 1). Generally, there is a strong spatial correlation between the density images of consecutive altitude intervals and the spatial correlation becomes weaker as two altitude intervals are apart. The spatial correlation is stronger for the consecutive altitude intervals above 2,001–2,500 ft (correlation coefficient is 0.80 and higher). The strongest correlation is between density images of 3,501–4,000 ft AGL and 4,001–4,500 ft AGL (correlation coefficient is 0.90); and 4,001–4,500 ft AGL and 4,501–5,000 ft AGL (correlation coefficient is 0.90).

The distribution of the waypoints from 0 to 5,000 ft AGL altitudes with an interval of 500 ft is shown in Figure 15. The majority of the waypoints are above the southwestern side of the park. The pattern of distribution of the waypoints showed that flights were also present at relatively lower AGL altitudes (purple dots) within the 0.5-mile boundary of the park especially above the southeastern side of the park. There are scattered circular flight patterns observed above Haleakalā Crater.

Table 1. Spatial correlation matrix of Above Ground Level (AGL) altitude point densities.

AGL Altitude Interval	1	2	3	4	5	6	7	8	9	10
1. 0–500 ft	–	–	–	–	–	–	–	–	–	–
2. 501–1,000 ft	0.65	–	–	–	–	–	–	–	–	–
3. 1,001–1,500 ft	0.37	0.63	–	–	–	–	–	–	–	–
4. 1,501–2,000 ft	0.06	0.18	0.67	–	–	–	–	–	–	–
5. 2,001–2,500 ft	0.01	0.06	0.40	**0.80**	–	–	–	–	–	–
6. 2,501–3,000 ft	0.01	0.04	0.28	0.55	**0.85**	–	–	–	–	–
7. 3,001–3,500 ft	0.01	0.02	0.17	0.33	0.56	**0.86**	–	–	–	–
8. 3,501–4,000 ft	0.01	0.01	0.09	0.17	0.31	0.58	**0.86**	–	–	–
9. 4,001–4,500 ft	0.01	0.01	0.05	0.08	0.16	0.36	0.64	**0.90**	–	–
10. 4,501–5,000 ft	0.01	0.01	0.03	0.04	0.08	0.21	0.41	**0.69**	**0.90**	–

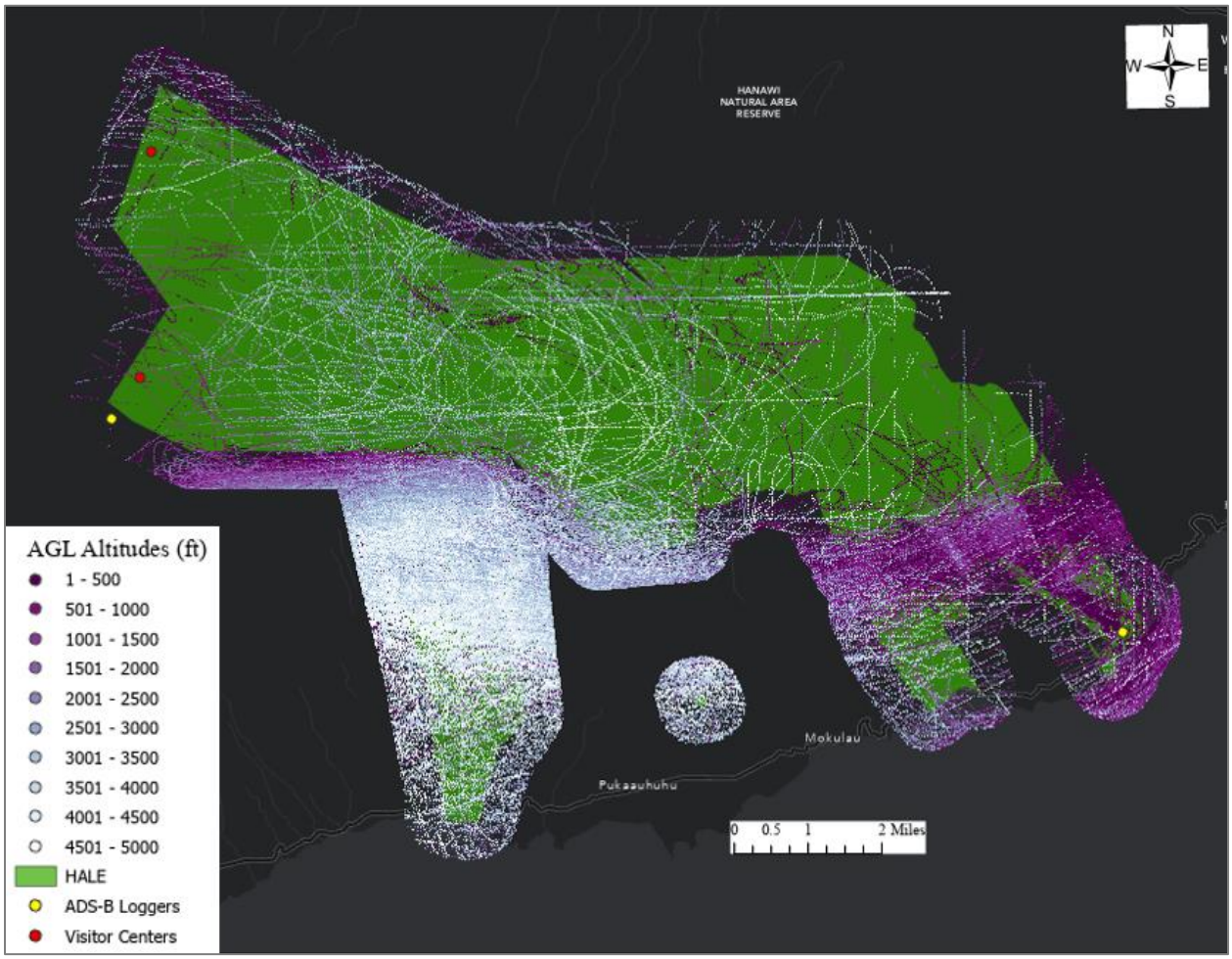

Figure 15. AGL altitude trends of altitudes ranging from 0 to 5,000 ft AGL for waypoints within 0.5 miles of the HALE boundary (*n* = 372,671 waypoints). NPS / BIJAN GURUNG

Waypoints with AGL altitude values less than 0 ft within the 0.5-mile boundary of HALE are shown in Figure 16. Any tracking point with a negative AGL is due to error, although identifying the exact error can be difficult. Broadly, error sources could be aircraft flying exceptionally low (including for landings or drop-offs) combined with DEM generalization errors and errors between barometric altitude estimates and actual altitude. The negative AGL values constituted only a small fraction of the overall waypoints and no consistent patterns are revealed in Figure 16.

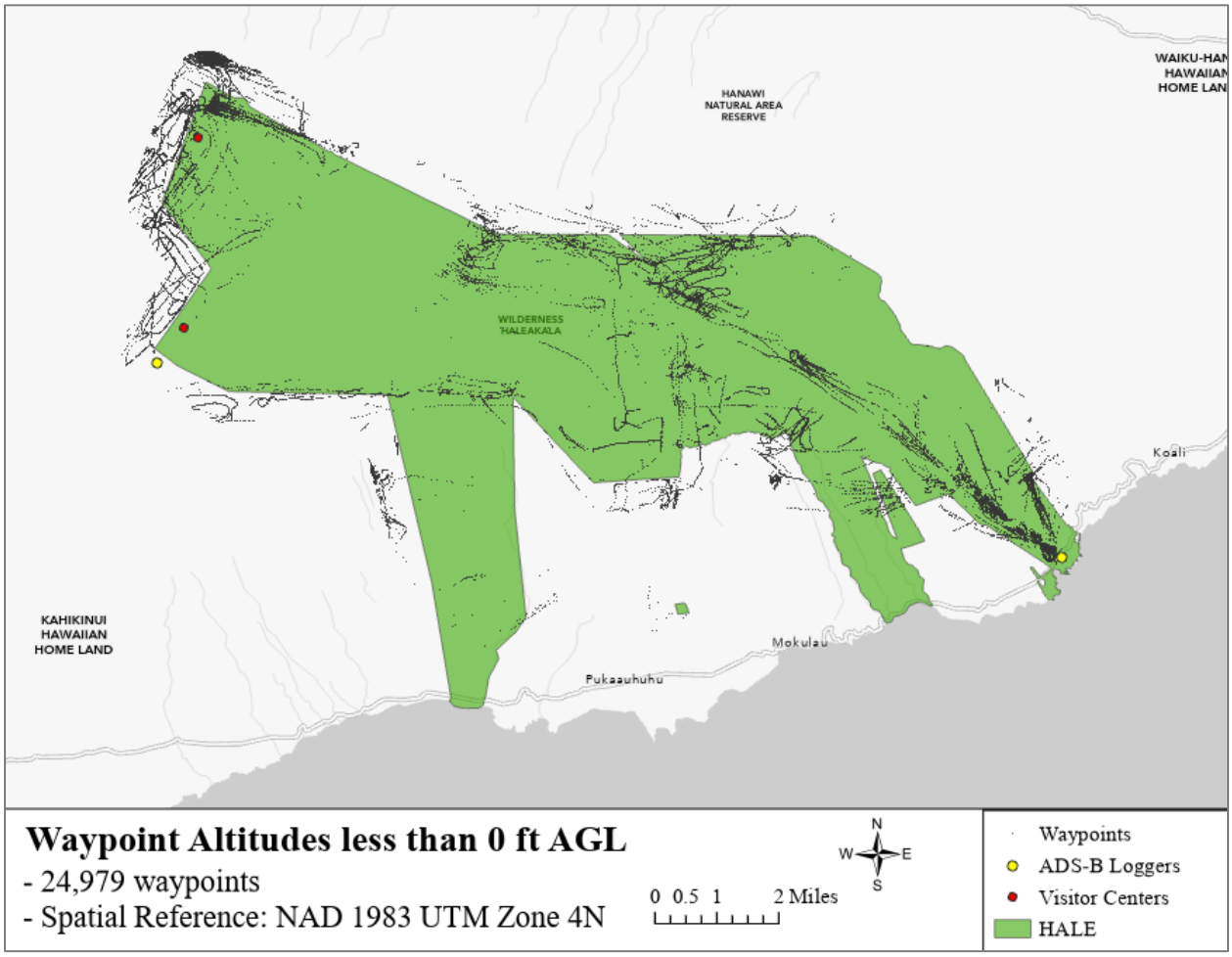

Figure 16. Waypoints with AGL altitude less than 0 ft AGL within 0.5 miles of HALE boundary (*n* = 24,979). NPS / BIJAN GURUNG

Figure 17 shows waypoints in altitudes from 0–12,500 ft MSL with an interval of 1,000 ft. Waypoints at the higher MSL altitudes are above the southwestern side of the park and the waypoints at lower MSL altitudes are above the southern side of the park, especially above Kīpahulu area, Kaʻāpahu region, and Nuʻu region. This trend follows the topography of the area.

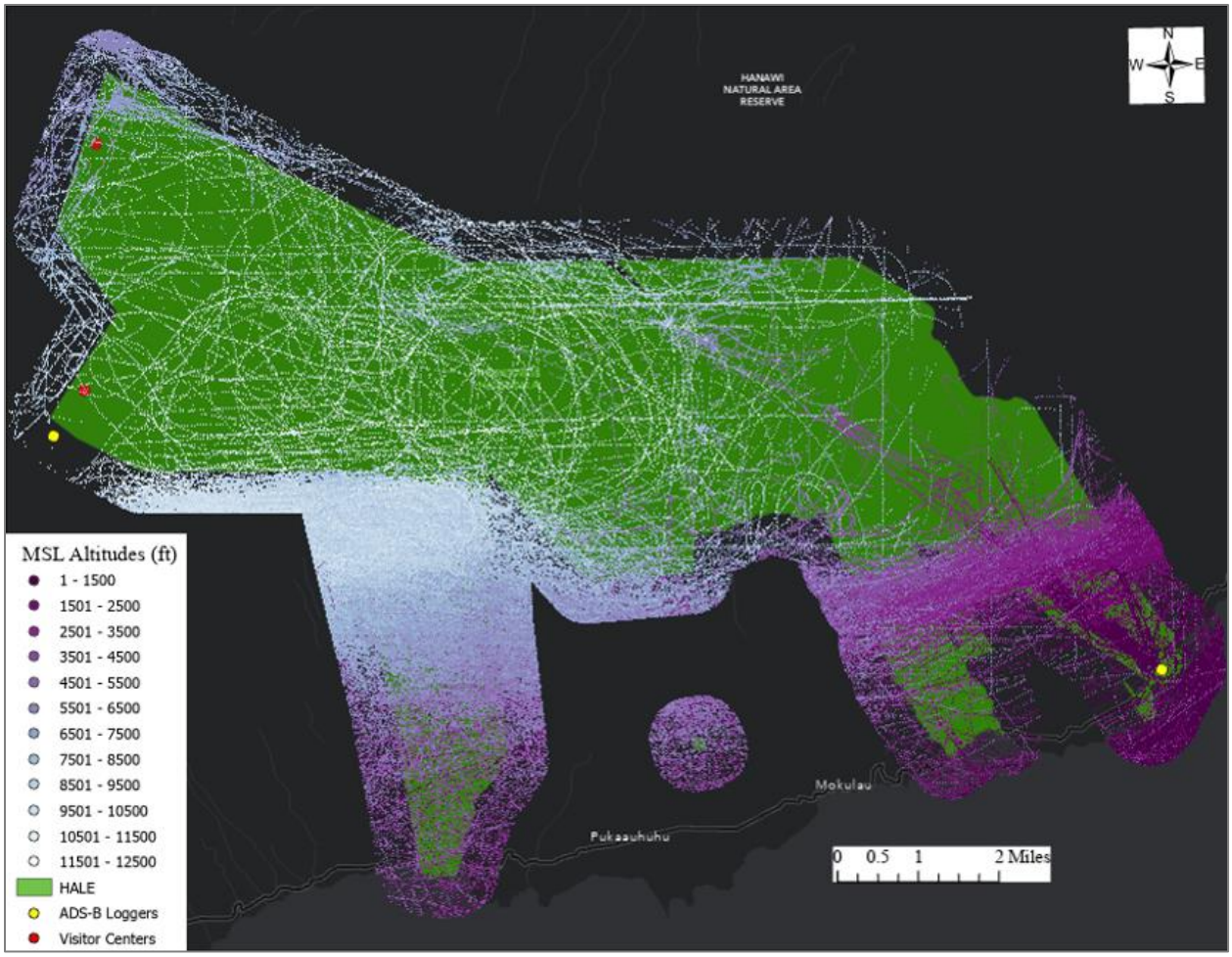

Figure 17. MSL altitude trends of altitudes ranging from 0 to 12,500 ft MSL for waypoints within 0.5 miles of the HALE boundary (*n* = 485,627 waypoints). NPS / BIJAN GURUNG

The distribution of waypoints across the AGL altitudes and MSL altitudes is shown in the tables below. The waypoints are distributed more or less uniformly in the ten AGL altitude categories but higher numbers are in the AGL altitude from 2,501–4,000 ft (Table 2). The waypoints are in higher numbers in the upper MSL altitudes (6,501–10,500 ft MSL) than in the lower MSL altitudes or above 10,501 ft MSL altitudes (Table 3).

Table 2. Number and percentage of waypoints across AGL altitude intervals (*n* = 397,650).

AGL Altitude	Number of Waypoints	Percentage of Waypoints
< 0 ft	24,979 [A]	6.28
0–500 ft	35,330	8.88
501–1,000 ft	30,626	7.70
1,001–1,500 ft	24,515	6.16

Table 2 (continued). Number and percentage of waypoints across AGL altitude intervals (*n* = 397,650).

AGL Altitude	Number of Waypoints	Percentage of Waypoints
1,501–2,000 ft	27,505	6.92
2,001–2,500 ft	39,567	9.95
2,501–3,000 ft	47,850	12.03
3,001–3,500 ft	48,293	12.14
3,501–4,000 ft	44,712	11.24
4,001–4,500 ft	39,756	10.00
4,501–5,000 ft	34,517	8.68

[A] 46.9% of these waypoints were from a single rotorcraft; three rotorcrafts constituted 87.9% of these waypoints.

Table 3. Number and percentage of waypoints across MSL altitude intervals (*n* = 485,627).

MIS Altitude	Number of Waypoints	Percentage of Waypoints
0–1,500 ft	22,932	4.72
1,501–2,500 ft	19,550	4.03
2,501–3,500 ft	28,879	5.95
3,501–4,500 ft	17,258	3.55
4,501–5,500 ft	16,352	3.37
5,501–6,500 ft	36,778	7.57
6,501–7,500 ft	54,293	11.18
7,501–8,500 ft	59,804	12.31
8,501–9,500 ft	132,970	27.38
9,501–10,500 ft	83,295	17.15
10,501–11,500 ft	12,607	2.60
11,501–12,500 ft	909	0.19

Low-level overflights were analyzed across months, days of the week, and hours of the day (total flights analyzed = 4,098). Table 4 shows the number of days data were collected per month, overflights per month, and the average number of flights per day for the data collection duration, which occurred from June 3, 2020, to March 31, 2023. The total number of days in Table 4 is less than the total number of days data were collected. This is due to the data reduction used in phrase 3 to focus only on low-level flights without commercial commuter traffic, straight-line flights, and other flights described above. On some days (e.g., bad weather or low visibility) air tours may not operate but commuter jets still conduct flights. A short R-script was used to calculate the number of data collection days. HALE received the most low-level overflights in July 2022 (16 average number of flights per day) but there was only one day of data collected in July 2022. In June 2021, July 2021, and August 2021 there was an average number of 13 flights per day. There were gaps in data

recording days: one after January 2022 for more than a month and another after July 2022 for more than four months (shaded rows in Table 4).

Table 4. Number and percentage of overflights across months (*n* = 4,098).

Month	Number of Data Collection Days [A]	Number of Overflights	Average Number of Overflights Per Day
June 2020	12	18	2
July 2020	9	10	1
August 2020	15	24	2
September 2020	14	17	1
October 2020	17	32	2
November 2020	21	53	3
December 2020	31	91	3
January 2021	24	82	3
February 2021	26	80	3
March 2021	29	132	5
April 2021	29	192	7
May 2021	30	248	8
June 2021	30	392	13
July 2021	30	378	13
August 2021	30	396	13
September 2021	8	60	8
October 2021	16	162	10
November 2021	29	304	10
December 2021	5	21	4
January 2022	14	124	9
March 2022	27	276	10
April 2022	28	257	9
May 2022	3	8	3
June 2022	2	17	9
July 2022	1	16	16
December 2022	10	116	12
January 2023	26	239	9
February 2023	13	85	7
March 2023	27	268	10
Total	**556**	**4,098**	

[A] For some months, data collection did not occur every day because of technological failure. Some months data were not collected at all.

The analysis also generated the percentage of flights across days of the week (Table 5). The days of the week with the highest percentage of flights were Fridays (17.3%) and Thursdays (16.1%). Table 6 shows the percentage of overflights across hours of the day. Most overflights occurred from 9:00 am to 1:00 pm. Table 7 shows the percentage of overflights across aircraft types. Rotorcraft is the aircraft type most common among overflights at HALE with 92.7% of the total overflights. Fixed wing single engine constituted 3.6%, fixed wing multi engine constituted 0.3%, and "null" values or unknown with 3.5% of the total overflights.

Table 5. Percentage of overflights across days of the week.

Day of the Week	Percentage of Overflights
Monday	14.2
Tuesday	14.2
Wednesday	13.8
Thursday	16.1
Friday	17.3
Saturday	13.4
Sunday	11.1

Table 6. Number and percentage of overflights across hours of the day for weekdays (*n* = 3,095) and weekends (*n* = 1,003).

Hour	Percentage of Overflights
7:00am–8:00am	1.5
8:00am–9:00am	9.6
9:00am–10:00am	17.3
10:00am–11:00am	19.4
11:00am–12:00pm	11.6
12:00pm–1:00pm	11.7
1:00pm–2:00pm	7.4
2:00pm–3:00pm	5.8
3:00pm–4:00pm	7.6
4:00pm–5:00pm	4.6
5:00pm–6:00pm	2.0
6:00pm–7:00pm	0.6
7:00pm–8:00pm	0.4
8:00pm–9:00pm	0.2

Table 7. Percentage of overflights across aircraft type.

Aircraft Type	Percentage
Fixed wing single engine	3.6
Fixed wing multi engine	0.3
Rotorcraft	92.7

Three more figures were produced to show overflight travel patterns of three aircraft types. Figure 18 shows overflight travel patterns for rotorcraft. Figure 19 shows overflight travel patterns for fixed wing single engine aircraft. Figure 20 shows overflight travel patterns for fixed wing multi engine aircraft.

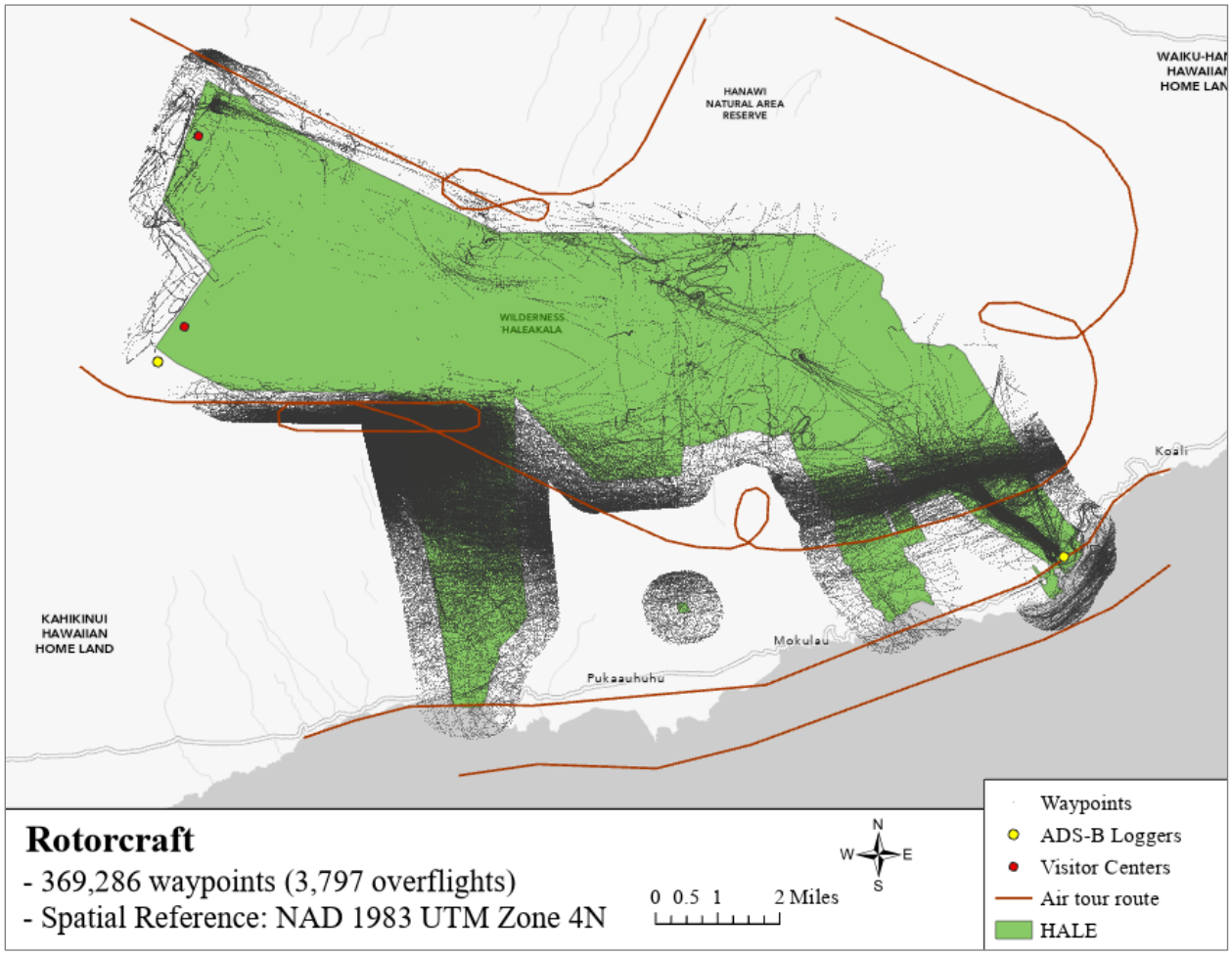

Figure 18. Rotorcraft overflight travel patterns. NPS / BIJAN GURUNG

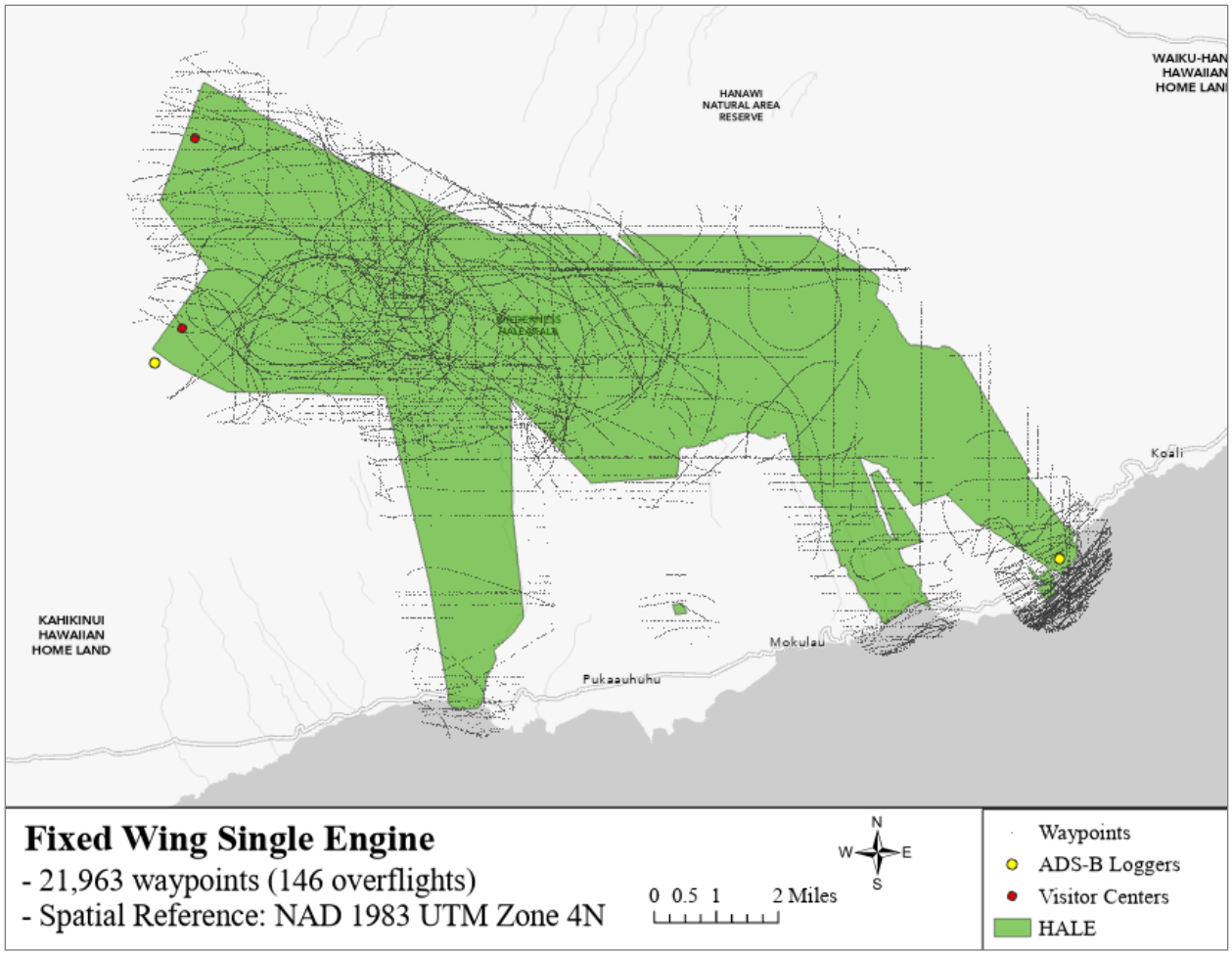

Figure 19. Fixed wing single engine overflight travel patterns. NPS / BIJAN GURUNG

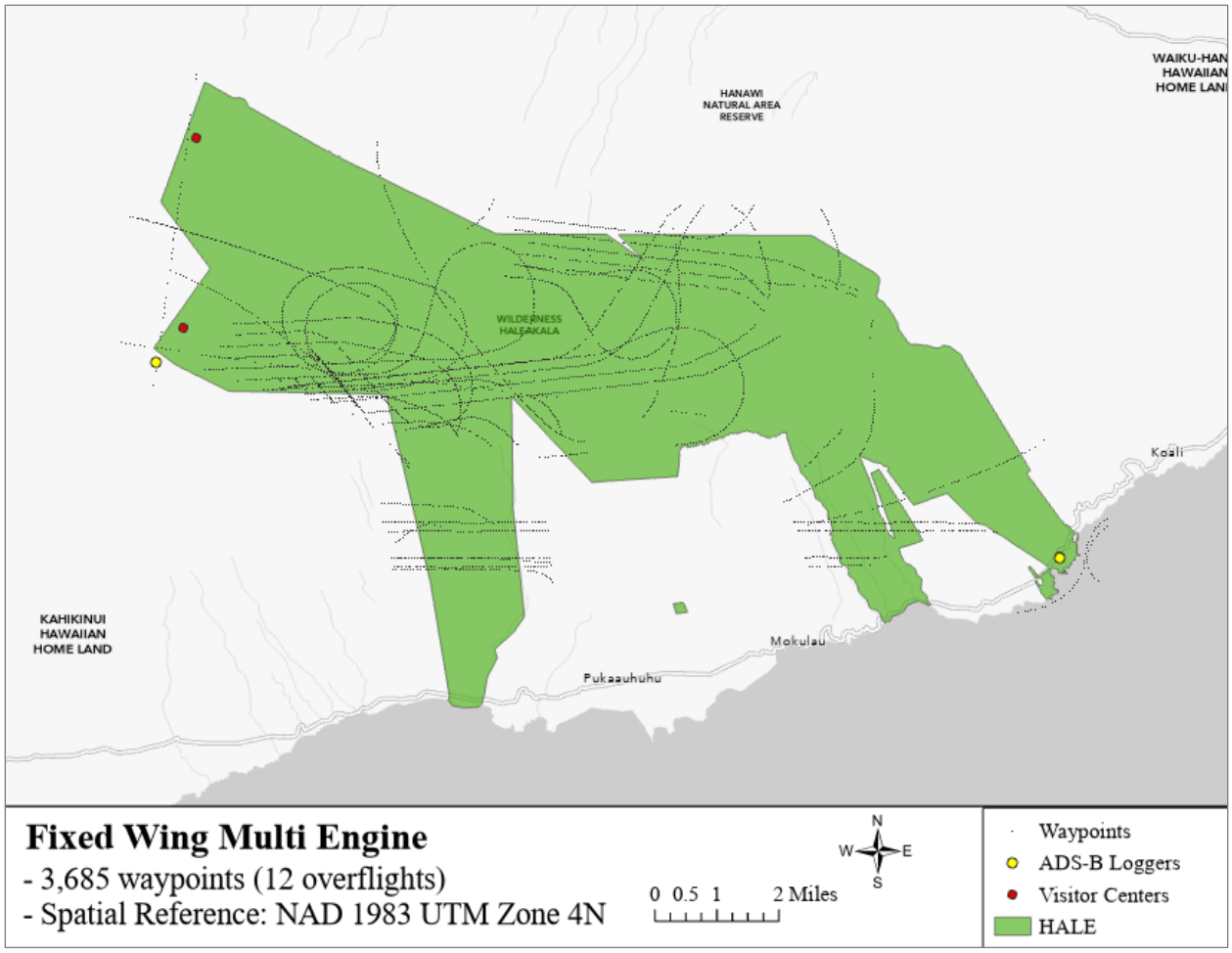

Figure 20. Fixed wing multi engine overflight travel patterns. NPS / BIJAN GURUNG

Discussion

The purpose of this study was to explore the spatial and temporal patterns of overflights over HALE by analyzing ADS-B data recorded from June 3, 2020, to March 31, 2023, with a total of 689 days of data collection by the data loggers. ADS-B data loggers were deployed at two locations: one near Haleakalā Summit (9,986 ft MSL) and another at Kīpahulu Visitor Center (113 ft MSL). The analysis consisted of 70,524 overflights that were analyzed across three phases.

The first phase focused on all overflights that flew within 10 miles of the park boundary. Overflights were concentrated along the major flight corridors of commercial airlines and followed a known air tour route south of the park. The majority of the flights, including commercial air tour operations, originate from Kahului Airport (class B airspace), which lies on the north-central part of Maui Island. Commercial air tours approach HALE from the west and south providing a view of the western and southwestern slopes of Haleakalā volcano and crater. Aircraft maneuver in this area to provide the best view and then proceed towards Kaupō Gap, Kaʻāpahu Region, and Kīpahulu district providing the view of waterfalls, dense vegetation, and coastline of Kīpahulu area (Figure 1).

The second phase of this analysis focused on low-level overflights. All waypoints below 12,500 ft MSL and within 10 miles of the HALE boundary were analyzed. Figures 4 and 5 represent the most holistic representation of these data, as these data were collected with both units working which provided the most robust spatial coverage. These figures mostly highlight how the majority of air traffic over the park is along a common air tour route: one from west to east along the southern edge of Haleakalā Crater which then flies along the south of the Kīpahulu area and one route that seems to stay along the coast, just outside of the park's southern boundary. The flight path along the southern edge of the Haleakalā Crater toward the Kaʻāpahu area was the main path of the air tours in previous studies (Beeco et al., 2020; Peterson, 2021). A few loops were detected around Haleakalā Crater and some parallel patterns of waypoints suggested survey flights (Figure 6 and Figure 8). While most flights on the island depart from Kahului Airport, there is also Hana Airport, with a single airstrip, which lies on the eastern part of Maui Island and this could be the reason for the concentration of overflights above this area (Figures 4-8).

The third phase focused on overflights within the 0.5-mile boundary of the park and below 5,000 ft AGL that have the most potential to impact the acoustic environment. These flights are the most likely to be air tours. Point density and kernel density analyses showed dense waypoints on the south side of the park, just south of the crater rim (Figures 10–14). Similar results were reported in the study by Peterson, 2021. However, the southwest side of the park received the maximum number of waypoints in the current analysis whereas Kīpahulu Visitor Center and Kīpahulu Campground received the maximum number of waypoints in the 2020 analysis (Peterson, 2021). This could be explained by the date during which ADS-B loggers were active. Kernel density analysis showed the highest density for the 2,501–3,000 ft AGL interval followed by the 2,001–2,500 ft AGL interval. The 2019 report also showed a similar flight path of air tours where they approached the park from the west, flew near the southern rim of the crater, made an "S" turn loop heading south, and then

progressed east toward Kīpahulu (Beeco et al., 2020). This reveals that the air tour travel patterns have been consistent across measurement years.

The spatial correlation is strong between the kernel density images of consecutive AGL altitude intervals and gradually becomes stronger as the interval increases (Table 1). Figure 15 shows the distribution of waypoints from 0–5,000 ft AGL altitudes with the concentration of waypoints above the southern part of the park, especially above the southern part of Haleakalā Crater (acoustic zone 2) and Kaupō Gap (acoustic zone 3), and Kīpahulu Coastal (acoustic zone 4). HALE was grouped into five acoustic zones based on vegetation cover, management purposes, etc. (Lee et al., 2016). The distribution of waypoints from 0–12,500 ft MSL altitudes showed a similar concentration of waypoints above the park (Figure 17). The distribution of waypoints in the ten AGL altitude categories showed the highest concentration of waypoints from 2,501–4,000 ft AGL altitude (Table 2). There is a concentration of waypoints above Nuʻu Region, as well (Figures 15 and 17). In acoustic monitoring at Nuʻu site in 2013, prominent noise sources included aircraft with a mean percentage time audible noise (in 24-hour time period) for aircraft as 25% (Job et al., 2016). The average number of overflights per day was higher in the summer months (Table 4) but was very low for the summer of 2020 probably due to the effect of the pandemic. The overflights began as early as 7 am and operated until 9 p.m. (Table 6). Rotorcraft was the most commonly used aircraft for low-level overflights (Table 7) which was similar to the findings shown in the previous study by Beeco et al., 2020. Rotorcraft overflights were mostly along the southern part of the park, following one of the recommended air tour routes, which includes the southern rim of the crater and the area south of Kīpahulu (Figure 18).

Negative values of AGL altitude of some waypoints are inherent in the ADS-B data analysis. In the Phase 3 analysis, waypoints with negative AGL values constituted 6.28% of the data (Figure 16). A single rotorcraft constituted 46.9% of the waypoints with negative AGL values, whereas three rotorcrafts constituted 87.9% of the waypoints with negative AGL values. These waypoints with negative AGL values are mostly distributed above Kīpahulu area and on the northwest side of the park. There is no specific pattern of these waypoints, but the fact that three rotorcrafts constituted 87.9% or four rotorcrafts constituted 95.6% of these waypoints with negative AGL altitude shows that these rotorcrafts may have been experiencing a malfunction with their ADS-B unit, calibration for barometric pressure, or some other issue. These negative AGL data were recorded over many days.

Finally, the newly finalized air tour management plan (ATMP) of Haleakalā National Park underscored a designated single one-way route from west to east along the southern area of the park and maintaining a minimum 2,000 ft AGL above land and 3,000 ft AGL over the ocean (National Park Service, 2024a). The ATMP was finalized in January 2024, whereas ADS-B data were collected before 2024. Thus, the park will likely experience a significant change in the overall aircraft travel patterns above the park (since a significant portion of flights above the park were likely air tours) post ATMP implementation in July 2024. We anticipate a shift to the newly designated commercial air tour route from 2024 onward as directed by ATMP (shown in Figure 1). The ATMP aims to reduce the sound levels (over a 12-hour day) by 30 decibels for the noise-sensitive regions of the

park, reduce the impact on endemic birds, reduce the impact on sacred sites, and improve the visitor experience in HALE (National Park Service, 2024a).

This study's results helped to understand low-level overflights, especially air tours at HALE in the years 2020–2023, and their potential to disrupt the natural soundscape. It would be interesting to compare these results with the results after the implementation of ATMP. This information can be used in the planning and management of parks to assist with conserving natural soundscapes, cultural landscapes, biodiversity, and the experience of terrestrial visitors.

Literature Cited

Beeco, J. A., & Joyce, D. (2019). Automated aircraft tracking for park and landscape planning. *Landscape and Urban Planning, 186,* 103–111. https://doi.org/10.1016/j.landurbplan.2019.03.001

Beeco, J. A., Joyce, D., & Anderson, S. (2020). Evaluating the Use of Spatiotemporal Aircraft Data for Air Tour Management Planning and Compliance. *Journal of Park and Recreation Administration*. https://doi.org/10.18666/JPRA-2020-10341

Hutchinson, J. M. S., & Peterson, B. A. (2023). *ADS-B Overflight Analysis Toolbox* (Version 1.0.1) [Computer software]. https://github.com/GISSAL/ads-b

Job, J. R., Pipkin, A. R., & Beeco, J. A. (2016). *Haleakalā National Park: Acoustic Monitoring Report* (Natural Resource Report NPS/NRSS/NSNS/NRR—2018/1678). National Park Service, Fort Collins, Colorado.

Lee, C. S. Y., Fleming, G. G., Roof, C. J., MacDonald, J. M., Scarpone, C. J., Malwitz, A. R., & Baker, G. (2016). *Haleakalā National Park: Baseline Ambient Sound Levels 2003* (DOT-VNTSC-FAA-06-09).

National Park Service. (2024a). *Final Air Tour Management Plan Haleakalā National Park*. https://parkplanning.nps.gov/document.cfm?documentID=133909

National Park Service. (2024b). Haleakalā Air Tour Management Plan (ATMP). https://parkplanning.nps.gov/projectHome.cfm?projectId=103365

National Park Service. (2024c). *Haleakalā National Park, Hawai'i*. https://www.nps.gov/hale/learn/nature/geology-guide.htm

National Park Service. (2024d). *National Park Service Visitor Use Statistics* [Dataset]. https://irma.nps.gov/Stats/Reports/Park/OLYM

Peterson, B. (2021). *Understanding overflights at Haleakalā National Park*.

United States Geological Survey. (2023). *The National Map – Data Delivery*. https://www.usgs.gov/core-science-systems/ngp/tnm-delivery

Volpe National Transportation Systems Center. (2004). *Haleakalā National Park: Air Tour Management Plan Planning and NEPA Scoping Document*. US Department of Transportation. https://rosap.ntl.bts.gov/view/dot/35551

National Park Service
U.S. Department of the Interior

Science Report NPS/SR—2025/224
https://doi.org/10.36967/2308068

Natural Resource Stewardship and Science
1201 Oakridge Drive, Suite 150
Fort Collins, CO 80525

NPS 162/195906, February 2025